6 Acoustic Impedance Measurements

Fig. 6.1 (previous page): First test of the mirror source set up and as expected is does not function as expected (2006).

6.1. Summay

In this chapter methods to determine the reflection (absorption) coefficient of acoustic materials are described. First some traditional methods are explained. After that three techniques to determine the reflection coefficient with the use of Microflowns are explained.

The first technique that involves Microflowns is similar to a current standardized method. Nowadays the reflection coefficient of acoustic samples is often determined in a standing wave tube with two closely spaced microphones. Here a method with a single pu probe in a standing wave tube is presented. This pu based method shows to be more accurate than the standardized methods [5]. However measurements in a tube have many disadvantages (it is destructive, bandwidth limited, only the normal reflection coefficient can be determined, there are errors due to the mounting of the material, results seem to be tube dependent, etc.). See further §6.4.

The second pu based method is the determination of the surface impedance [5] and with that the reflection coefficient, it is therefore called the surface impedance method. It is a fast and broad banded method that makes it also possible to determine the reflection coefficient under angles in situ. A model is used to convert the obtained spherical reflection coefficient into the required planar reflection coefficient.
With this method it is possible to measure the absorption of acoustic damping materials broad banded, in situ and under all angles, but the measurement of highly reflective surfaces and measurements in a confined place is difficult.

The last Microflown based method (the mirror source method) is capable of measuring highly reflective surfaces. It is an in situ method that makes use of a monopole sound source and a Microflown that is placed so that it is not sensitive in the direction of the monopole. It will therefore measure the 'mirror source' only. With this method it is possible to broad banded measure the absorption of also highly reflective materials in a confined placed like inside a car within seconds. The method is not fully understood yet. See further §6.9.

6.2. Introduction

In the previous chapter sound intensity (I), that has a close relation to the product of sound pressure and particle velocity, was discussed. In this chapter the measurement of the ratio of sound pressure and particle velocity is the focus of attention. The ratio of sound pressure at a point and the associated component of particle velocity is defined as the specific acoustic impedance (Z) at that point in a sound field.

Sound intensity is associated with the product of sound pressure and particle velocity and quantifies the amount of sound energy that propagates through a unit area. The specific acoustic impedance is related with the ratio of both, and is a useful quantity to determine for example the reflection or absorption of acoustic damping materials.

Sound energy density (E), which is related to the sum of the sound pressure and particle velocity, quantifies how much energy is "stored" in an acoustic wave, sound intensity quantifies how much sound energy is transported and specific acoustic impedance quantifies the possibility for sound energy to be transported.

Suppose that in a certain set up sound is travelling towards a full reflecting (rigid) surface and the acoustic impedance is determined close to that surface. The acoustic impedance will be high because close to the surface the particle velocity is almost zero and the sound pressure is enlarged due to the reflection. All the sound is reflected, an therefore close to the surface the intensity is zero: the same amount of sound that goes in one direction goes also in the opposite direction so there is no net flow of acoustic energy. The sound energy will not be affected much by the surface because compared to a free propagating sound wave, the sound pressure increases and the particle velocity decreases.

If the full reflecting (rigid) surface is removed, the acoustic impedance will change to the characteristic impedance of air ($Z=\rho c \approx 435 Nsm^{-3}$). The sound intensity will not be zero anymore and its value will depend on the loudness of the sound field. The sound energy will not alter.

Note that the impedance is not dependent of the loudness of the sound field; it is determined by the environment. Both sound intensity and sound energy is dependent of the loudness of the sound field.

Because the impedance is not influenced by the loudness of the sound it is easier to calibrate an impedance measurement setup than e.g. a sound intensity measurement setup or a single sound probe. Only a reduced calibration is required; this is a calibration without a reference microphone.

6.3. Techniques to determine the reflection coefficient

There are several techniques to determine the reflection coefficient of materials. They can be divided in three groups: measurements in a reverberant room, in a tube and free field techniques. The methods are discussed below.

A number of authors have proposed methods to measure the acoustic properties of sound absorbing materials under free field conditions. In general the methods are suited for measurements with oblique incident waves.

One known technique is for example the pulse technique. A short signal is generated and the direct and the reflected waves are separated to calculate the reflection coefficient. It is noted that the sample has to be placed outside the near field, which can pose a lower limit on the frequency band of interest, and on the dimensions of the samples (several m^2).

Another technique uses two microphones placed close to the sound absorbing surface. With this method it is possible to calculate the normal impedance at the surface for oblique incident waves.

The possibility to measure the acoustic behaviour of sound absorbing materials under oblique incident waves is a strong advantage of the free

field method. Oblique incident waves cause shear waves that propagate in the sound absorbing material. These waves cause a different acoustic behaviour.

Disadvantage of the traditional free field methods is that the setup to determine the acoustic properties of sound absorbing materials is very large and (thus) expensive. If the oblique impedance is determined, often a robot is used to move sensors.

Free field methods are the only way to find out the reflection coefficient at different angles but the traditional setups need a lot of space, use mostly a robot, need (semi) anechoic conditions and a lot of measurement time. Due to these requirements, it is difficult to perform in situ measurements.

Free field methods under (semi) anechoic conditions

In this chapter a Microflown based technique is presented that is capable to measure the acoustic impedance near to the surface (and related to that the reflection coefficient) of an acoustic material. The method allows both normal and oblique measurements and the mathematics to obtain measurement results are straightforward. Because the impedance is determined close to the surface, a small measurement area is required. The method is developed in cooperation with the university of Leuven [5], [6], [7].

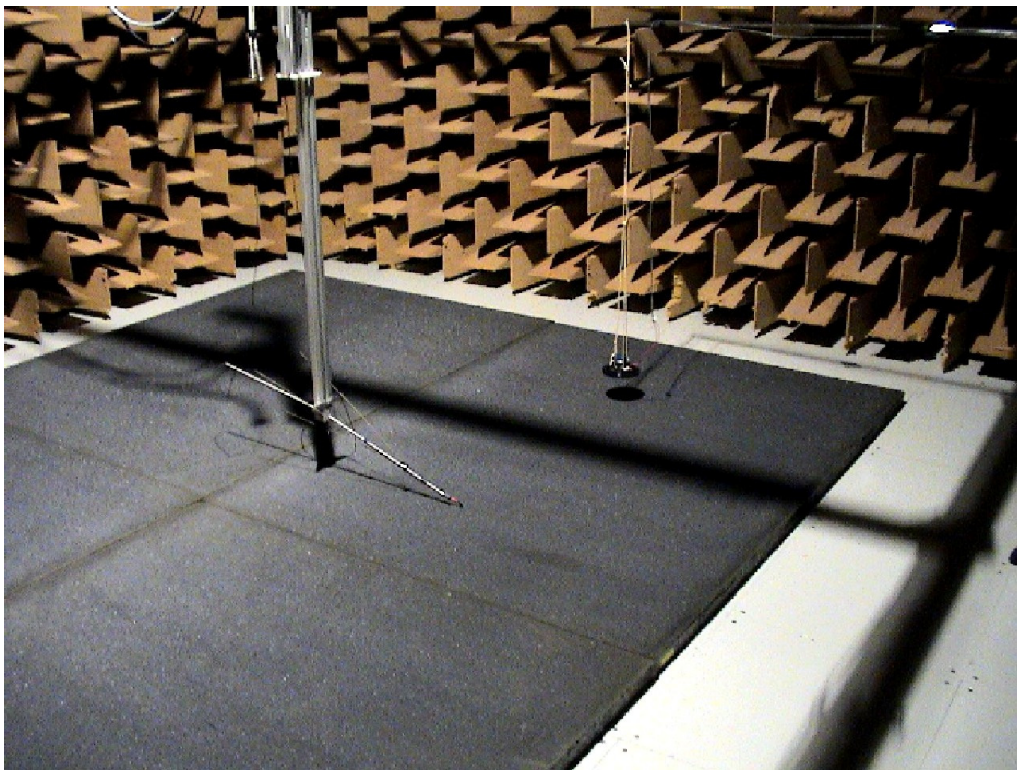

Fig. 6.2: Photograph of Tamura [26], [27] setup at the University of Leuven.

Before the Microflown based methods are presented, first some other known methods are treated.

Reverberant field method

The so-called reverberant field method is a well-known technique to measure sound absorption coefficients for random incident waves [1]. Experiments are performed in a reverberation chamber in which a diffuse sound field is generated. Diffuse field absorption coefficients are a key issue for the development of noise control treatments using simulation tools.

There are a number of standards available for the procedures as well as for the geometry and dimensions of the test chambers. A known set up is the Alpha cabin. It is a reverberation chamber having linear dimensions one-third of those of an international standard reverberation room. Its volume is 6.4m^3 and no two walls are parallel. As a result of the size reduction of the room, the sample surface area is reduced to 1.2m^2 an area that corresponds to that of typical hood- and roof-liners (typical size in a standard room is in the order of 10m^2). The measurement frequencies are also increased proportionally, so that the useful range lies between 400 and 10kHz [9].

Fig. 6.3: A Rieter Alpha cabin [9].

Usually a (diffuse) sound field is generated with a uniform energy density. This is achieved with loudspeakers that are placed in the corners of such chambers and a number of diffusers to prevent the presence of standing waves in the chamber. A relatively large sample of the sound absorbing material (several m^2) is placed in the chamber and for a given frequency band the reverberation time T_{60} is measured. T_{60} is the elapsed time at which the sound pressure level has dropped 60dB after the shutdown of the loudspeakers. The same procedure is performed without the sample and the difference is a measure for the absorption coefficient.

For highly sound absorbing materials, the absorption coefficient can exceed a value of one because of extra energy loss due to edge effects and diffraction. This can also be the case if the sound field is non-diffuse. Various standards state that at least 20 modes of vibration in the chamber are required in the lowest frequency band. As a result the room volume must be quite large. Nevertheless considerable differences have been observed for measurements on the same test materials in different reverberation chambers.

It has been shown that if the total energy (that is the pressure plus the velocity vector) is measured, the accuracy of the measurements increases [33].

Impedance tube methods

Although a number of measurement techniques can be used to quantify the sound absorbing behaviour, most often the determination of the properties takes place in a standing wave tube. This is because in a tube the mathematic problem becomes one-dimensional (in a certain bandwidth): sound waves can only propagate in one direction. This makes the experimental set-up relatively simple and small. In Fig. 6.4 a sketch of two basic techniques is shown.

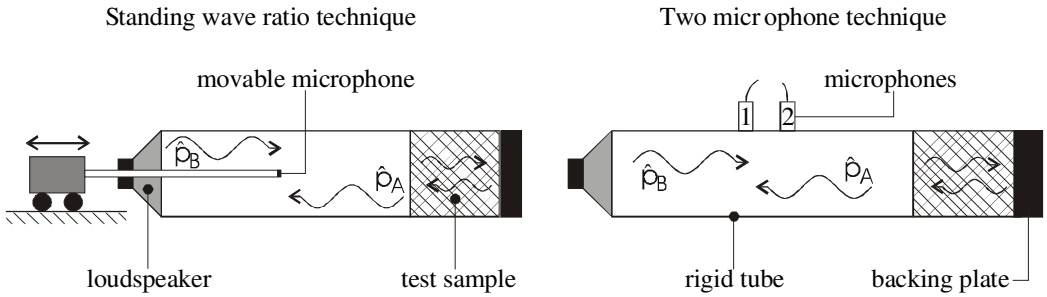

Fig. 6.4: Schematic representation of two measurement techniques in an impedance tube.

At the left-hand side a loudspeaker is placed and at the opposite side a sample of the test material is placed. In the tube a standing wave pattern is formed, being the result of a forward travelling sound wave $\hat{p}_A$, and a backward (or reflected) sound wave $\hat{p}_B$. The frequency of the sound waves is kept lower than the cut-off frequency to assure the generation of plane propagating waves in the tube.

The reflection coefficient of the test sample at the end of the tube can be determined if the forward travelling sound wave and reflected sound wave can be measured separately. This can be done with several methods which are discussed below.

Two microphone standing wave tube methods

In 1980 Chung and Blazer [17], [18] presented a technique which is based on the transfer function of two fixed microphones which are located at two different positions in the tube wall (see right-hand side of Fig. 6.4)

[1]. This method will be called the **2p method**. The standing wave pattern is built up from a broadband stationary noise signal. With the measured transfer function, incident and reflected waves are separated mathematically. This leads to the reflection coefficient of the sample for the same frequency band as the broadband signal. The impedance and absorption coefficient can be derived as well. The method is as accurate as the SWR method (see below) and considerably faster. The transfer function method has proven to be reliable and has been standardised (ISO 10534-2, 1998).

In practical setups three microphones are used to increase the frequency range. At lower frequencies a larger spacing is used.

Analogously to the 2p method it is also possible to use particle velocity sensors to determine the impedance *Z* (**2u method**) [3]. Again the transfer function between the two (particle velocity) microphones is dependent on the acoustic impedance *Z,* the spacing between both sensors and the distance between the sample and the sensors. The 2u method has the same disadvantages as the 2p method and therefore it has no practical use.

It is also possible to use a combination of a sound pressure probe and a particle velocity sensor and to measure the impedance in the tube in a direct manner. This method is in fact almost the same as the 2p and 2u method: the acoustic impedance is measured in the tube and then the acoustic impedance at the end of the tube is calculated. We will call this the **p/u method.** Because the p/u method makes no use of the sound gradient (like the 2p and the 2u method) this method performs good at lower frequencies. The method is discussed below in more detail (§6.4).

One microphone impedance tube methods

Earlier techniques made use of the measured standing wave ratio (SWR) for a specific frequency in the tube. By means of a movable microphone the ratio of the pressure maximum to the pressure minimum is determined. This ratio is then used to calculate the reflection coefficient and the acoustic impedance. An advantage of this method is that it is not necessary to calibrate the microphone. Drawbacks are the complex set-up with a movable probe and time needed to find the maximum and minimum pressure for *each* frequency of interest [2], [11].

Another method that uses only one microphone or Microflown is a repeated measurement with an altered sensor position using two times the same input signal. The sensor signals are stored in a computer and synchronised in post-processing in such way that the measurement seems to be performed with two sensors at the same time in stead of with one sensor in two times.

Drawbacks of impedance tube methods

First of all the method is destructive, it is not possible to measure the acoustic materials in situ and only the normal reflection coefficient is determined.

Some authors advise the use of acoustic properties which are independent of the test configuration such as the characteristic impedance and the propagation coefficient in the material. One technique to derive these two coefficients is to measure the surface impedance of the material with two different thicknesses.

For low frequencies the impedance tube method may not give accurate results because an airtight fit of the sample is needed and at the same time the sample has to be able to vibrate freely (and the pressure gradient becomes too low for the 2p method). This may also be a problem for higher frequencies when laminated materials or materials covered with a screen (for example a perforated sheet) are used. Furthermore, for a non-zero transverse contraction ratio (Poisson's coefficient) it is unlikely that a small sample is representative for a large area.

The tube has a high frequency limitation caused by the cut-off frequency of the tube that is proportional to the inverse of the tube diameter, see Eq. (6.1). Upper frequency limits are in the order of 4kHz (with a 5cm tube).

Obviously only the normal (perpendicular to the surface) sound properties can be measured in the tube. Therefore only materials that are locally reacting can be measured in the tube. "Locally reacting' means that the damping properties of the material do not change with the angle of incidence. For practical materials it shows that this is normally not the case. A measurement of the absorbing properties in the normal direction is therefore not sufficient. Only a measurement of the damping properties in all directions is conclusive; a tube measurement does not comply in most practical cases.

Only materials with uniform spatial properties can be measured in a tube because the rigid walls of a tube reflect the sound field so that only plane waves propagate. A measurement of a single quarter lambda resonator in the end plate will result on in a value that can be compared with a free field measurement of an infinite plate with multiple (also an infinite number) of quarter lambda resonators with a certain spatial distribution. The distribution of these virtual resonators is depending on the tube shape and dimensions.

The influence on the acoustic sample of the rigid tube wall can not always be ignored. In the paragraph 6.5, 'PU Kundt's tube vs. free field measurements', these differences are shown. The errors due to the tube influence are also known in literature [30]: materials with a high flow resistivity vibrate in reaction on a sound field. The vibration in the tube causes friction losses and that causes the measured damping properties to change. This is a very unwanted effect that cannot be solved.

Experts state that no reliable measurements can be done in a tube and that free field measurements are required.

6.4. The Microflown in the Kundt's tube

The impedance tube is used to determine the sound absorbing characteristics of materials like glass-wool or foams. In the tube a one-dimensional acoustic field is generated with a speaker. The plane waves are

reflected and absorbed by the sample material at the end of the tube. The reflection coefficient R or the absorption coefficient $\alpha=1-|R|^2$ can be calculated from the acoustic impedance Z. All quantities, R, α and Z are frequency dependent.

Here only the basic theory will be explained. The viscosity and the thermal conductivity of the fluid affect the wave propagation. Due to this, the measurement results will be a few percent underestimated. More correct models are presented in e.g. [1], [4], [6].

In a tube, above the cut-off frequency the specific acoustic impedance changes due to the existence of standing waves perpendicular to the direction of the sound wave. The set-up will then be very difficult to use since the acoustic impedance is not real and constant anymore. Tubes are only used below the cut-off frequency. For a cylindrical tube this cut-off frequency is given by:

$$f_c = \frac{c}{1.71 \cdot d} \tag{6.1}$$

Where d represents the diameter of the tube, and c the speed of sound (approximately 330m/s).

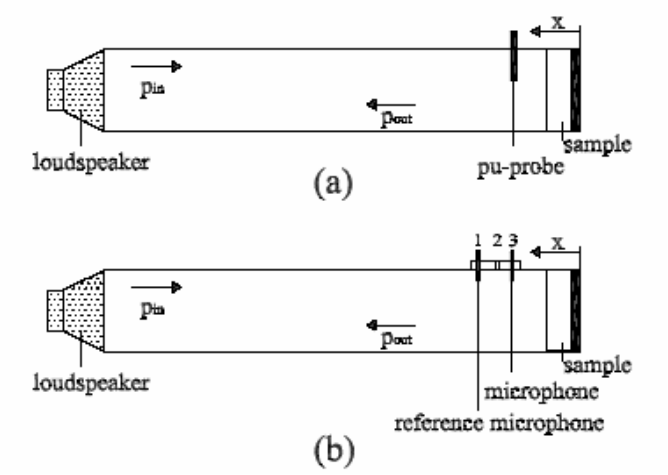

Fig. 6.5: Schematic representation of two measurement techniques in an impedance tube.

In the tube a one-dimensional acoustic field is generated with a speaker placed at one end of the tube. The sound wave that is generated by the sound wave is given by:

$$p_{in}(x,t,\omega) = p_0 \; e^{i(\omega t + kx)} \tag{6.2}$$

with $k=\omega/c_0$. The sound wave from the loudspeaker is reflected by the acoustic material. This wave is the resulting wave after phase rotation and attenuation of the incoming wave at the sample surface. The reflected wave is then given by:

$$p_{out}(x,t,\omega) = p_0 \; R(\omega) e^{i(\omega t - kx)} \tag{6.3}$$

The reflection coefficient is frequency dependent. In the tube, a standing wave is established as a result of the incoming and outgoing wave. The resulting pressure field in the tube can be described by:

$$p_{tot}(x,t,\omega) = p_{out}(x,t,\omega) + p_{in}(x,t,\omega) = p_0 \left(e^{i(\omega t+kx)} + R(\omega) e^{i(\omega t-kx)}\right) \tag{6.4}$$

From the equation of momentum conservation, the particle velocity in the tube can be derived:

$$u_{tot}(x,t,\omega) = \frac{1}{\rho_0}\int \frac{\partial p_{tot}(x,t,\omega)}{\partial x} dt = \frac{p_0}{\rho_0 c} \left(e^{i(\omega t+kx)} - R(\omega) e^{i(\omega t-kx)}\right) \tag{6.5}$$

The impedance at a position *x* in the tube is given by:

$$Z(x,\omega) = \frac{p_{tot}(x,\omega)}{u_{tot}(x,\omega)} = \rho_0 c \frac{e^{ikx} + R(\omega) e^{-ikx}}{e^{ikx} - R(\omega) e^{-ikx}} \tag{6.6}$$

So, if sound pressure and sound particle velocity at a distance x from the sample surface is known, the reflection coefficient and surface impedance of that sample can immediately be deduced:

$$R(\omega) = e^{2ikx} \frac{Z(x,\omega) - \rho_0 c}{Z(x,\omega) + \rho_0 c} \tag{6.7}$$

The acoustic absorption coefficient of the sample can be calculated by:

$$\alpha(\omega) = 1 - \left|R(\omega)\right|^2 \tag{6.8}$$

The surface impedance is given by:

$$Z(0,\omega) = \rho_0 c \frac{1 + R(\omega)}{1 - R(\omega)} \tag{6.9}$$

The most common way nowadays to determine the specific acoustic impedance in the tube is to use two pressure microphones (2p method) [17]. In this method the ratio of the output signals of the pressure microphones used to determine the properties of the sample. A similar method (2u method) that operates with two particle velocity microphones is explained as well in this paragraph.

By measuring the velocity at two distinct points in the tube a transfer function, $H_{2u}=u_2/u_1$, can be calculated [3]. From the transfer function H_{2u} the reflection coefficient of the sample material can be derived. The two positions in the tube where the velocity is measured are given in Fig. 6.5, at a distance $x=L$ and at a distance $x=L-s$ from the sample (the two microphones are spaced by a distance s).

$$H_{2u}(\omega) = \frac{S_{u_1 u_2}}{S_{u_1 u_1}} = \frac{e^{ik(L-s)} - R\ \ e^{-ik(L-s)}}{e^{ikL} - R\ \ e^{-ikL}} \tag{6.10}$$

S_{u1u2} is the cross-spectrum of both probes and S_{u1u1} the auto-spectrum of probe $\boldsymbol{u}_1$. Rewriting the transfer function H_{2u} results in an expression for the reflection coefficient at the sample material (x=0):

$$R(\omega) = \frac{e^{ik(L-s)} - H_{2u}(\omega)e^{ikL}}{e^{-ik(L-s)} - H_{2u}(\omega)e^{-ikL}} \tag{6.11}$$

Analogously to the ratio of the velocities measured at x=L and x=L-s, it is possible to define a quotient of p_1 and p_2, yielding:

$$H_{2p}(\omega) = \frac{S_{p_1p_2}}{S_{p_1p_1}} = \frac{e^{ik(L-s)} + R \quad e^{-ik(L-s)}}{e^{ikL} + R \quad e^{-ikL}} \tag{6.12}$$

where p_1 and p_2 represent the measured pressures at x=L and x=L-s.

Applying some mathematics, it can be deduced that there is a mutual and unique relation between H_{2u} and H_{2p}, i.e.

$$H_{2u} = \frac{(1+e^{2iks})H_{2p} - 2e^{iks}}{2e^{iks}H_{2p} - (1+e^{2iks})} \tag{6.13}$$

Expression (6.13) shows that, since H_{2u} and H_{2p} are uniquely related and only the spacing s (not even L) appears, the 2u and 2p-method are not fundamentally different.

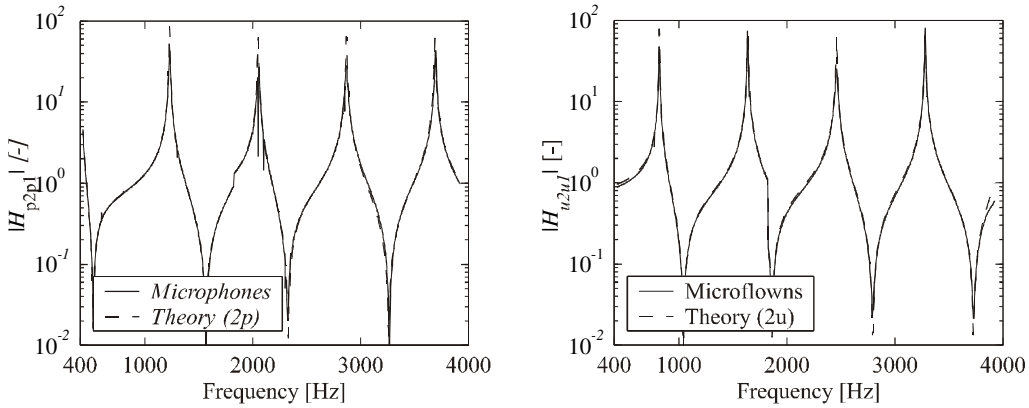

Fig. 6.6: Transfer functions H_{2p} and H_{2u} for an acoustic hard wall using the 2p and the 2u method.

From the viewpoint of determining the ratio H, both methods can be used. Fig. 6.6 shows the measured signals such as defined above for an acoustic hard wall. As can be seen the signals are quite similar and have a dynamic range of about 10,000 (80dB).

The signals that are displayed in Fig. 6.6 are used to calculate the reflection coefficient that should be unity (acoustic hard wall). The result is shown in Fig. 6.7.

For both methods the experimental results correspond to the theoretical reflection coefficient of $|R|=1$, except for the higher frequencies some deviations can be seen.

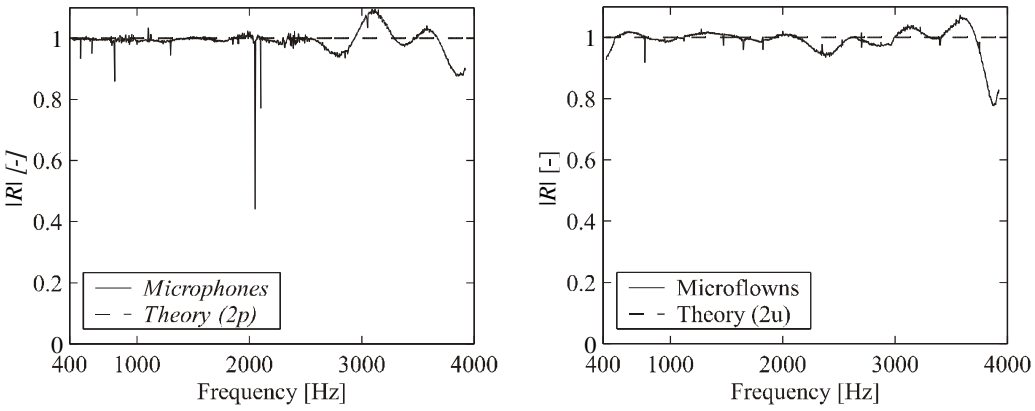

Fig. 6.7: Reflection coefficient of an acoustic hard wall using the 2p and the 2u method.

A reflection coefficient $|R|>1$ indicates inaccuracies in the measurements for higher frequencies. The calculation of R for a hard wall is relatively sensitive to these inaccuracies. This is explained by the sensitive transformation of the measured transfer function, which ranges theoretically from $+\infty$ to $-\infty$, to the reflection coefficient of $R=1$. This causes numerical problems and incorrect values of the impedance.

PU based Kundt's tube, Ratio of intensity and energy

This p**-u** method is determining the reflection coefficient with a slightly different approach [4]. Imagine the sample in the tube is full sound reflecting: all the sound that is put into the tube will be reflected at the end. The sound intensity (the net flow of sound energy in one direction) in the tube will be zero due to this. If on the other hand the sample is fully sound absorbing, the sound intensity will be a large figure. How large this figure is depends (apart from the absorption) on the amount of noise that is generated by the loudspeaker. The loudness can be determined by other acoustic quantity, the sound energy density.

This expression is independent on the place but, however, dependent on the driving sound pressure of the loudspeaker. To be able to determine the amount of sound that is generated by the loudspeaker, an alternative method therefore is utilised based on the so-called sound energy density E.

The ratio of the sound intensity and the sound energy density in the tube is given by:

$$\frac{\bar{I}_a}{E} = \frac{Re\{S_{pu}\}}{\frac{S_{pp}}{2\rho_0 c^2} + \frac{1}{2}\rho_0 S_{uu}} = c \cdot \frac{1-|R|^2}{1+|R|^2} \tag{6.14}$$

Comparison PU based tube measurement 2p and pu method

A known material was measured using the traditional method and the pu method [6]. The results of a measurement of the porous material in a Kundt's tube with diameter of 3.9cm and the pu-probe placed at a distance of 2.5cm from the sample surface are depicted in Fig. 6.8. A good correspondence between the simulated curve and the pu-technique is reached.

A second measurement is also shown in this figure. This measurement is done by measuring the sound pressure at two positions in the tube, called the 2p-technique (in figure denoted as pp-technique). The dip in this measurement curve is due to the fact that one of the microphones lies at a pressure minimum at that frequency.

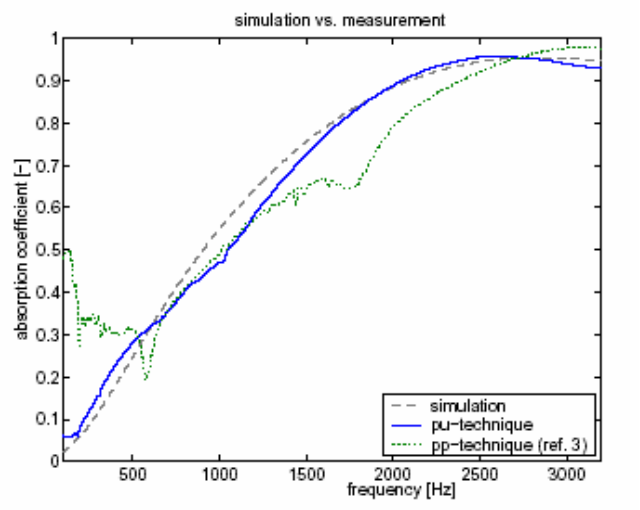

Fig. 6.8: Kundt's tube measurement, simulation vs. measurements [6].

PU based Kundt's tube method, an example measurement

The first step of the pu Kundt's tube method is the reference measurement that is done with no sample at the end of the tube. So the pu probe is put airtight at the side of the tube and the tube is closed with a fully reflecting plate. The amplitude response of the transfer function ($Z_{uncorrected}=S_{pu}/S_{uu}$) is shown in Fig. 6.10 (black line).

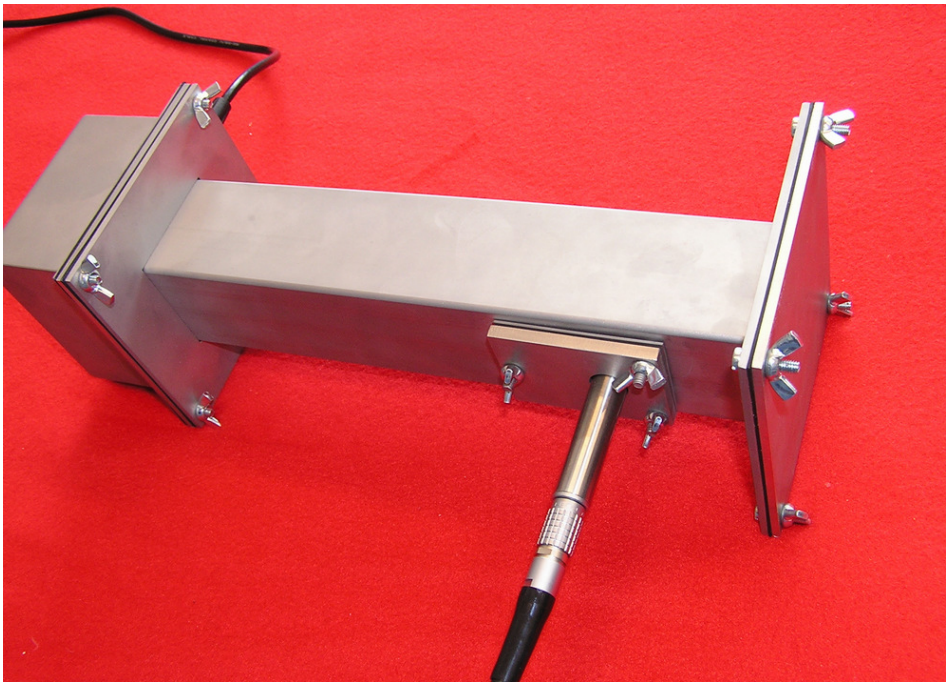

Fig. 6.9: The small standing wave tube is modified so that it becomes a pu based Kundt's tube.

Then the tube is opened, an acoustic sample is placed in at the end and the tube is closed again. The amplitude response of the transfer function ($Z_{uncorrected,\ sample}=S_{pu}/S_{uu}$) is shown in Fig. 6.10 (grey line).

The frequency f_u is found at the velocity minimum (so the maximum at 3263Hz) and f_p the is found at the pressure minimum (that is the first minimum at 1494Hz).

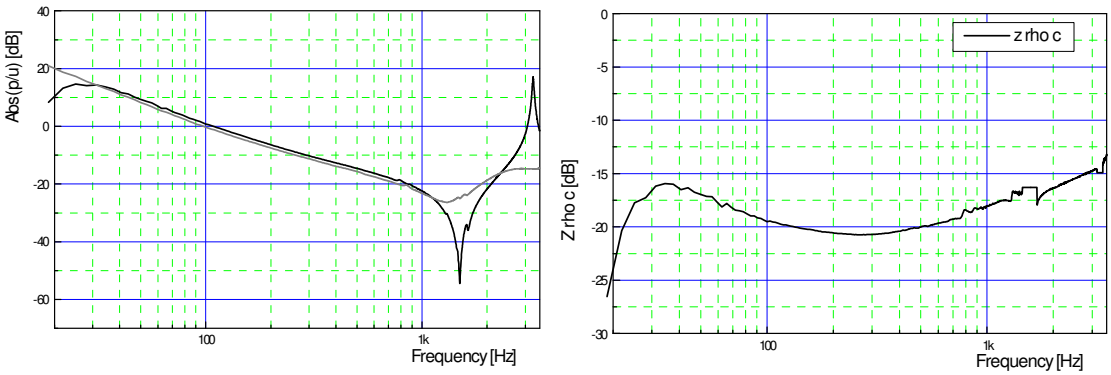

Fig. 6.10 (left): Amplitude response of the uncorrected impedance. Black line: rigid termination, grey line response with an absorbing sample at the end of the tube. Fig. 6.11 (right): The measured impedance in a tube. This response is similar to the free field response. At the frequencies f_u and f_p the response is estimated using interpolation.

The measured impedance in the tube is shown in Fig. 6.11. This response is similar to the free field response, so the response as if the probe was measuring a plane wave or in an anechoic room far from the source. At the

frequencies f_u and f_p the response is measured not accurately. Therefore the response around these frequencies is estimated by interpolation.

The amplitude response of the uncorrected impedance (black line Fig. 6.10) can be converted in the free field response (Fig. 6.11) by:

$$Z_{ff} = Z_{tube,rigid} \frac{\sin(\pi \frac{f}{f_u})}{\cos(\frac{\pi}{2} \frac{f}{f_p})} \tag{6.15}$$

The normalised impedance of the sample is given by the ratio of the measured response of the sample in the tube (as shown in Fig. 6.10, grey line) and the free field response (as shown in Fig. 6.11). The result is given in Fig. 6.12.

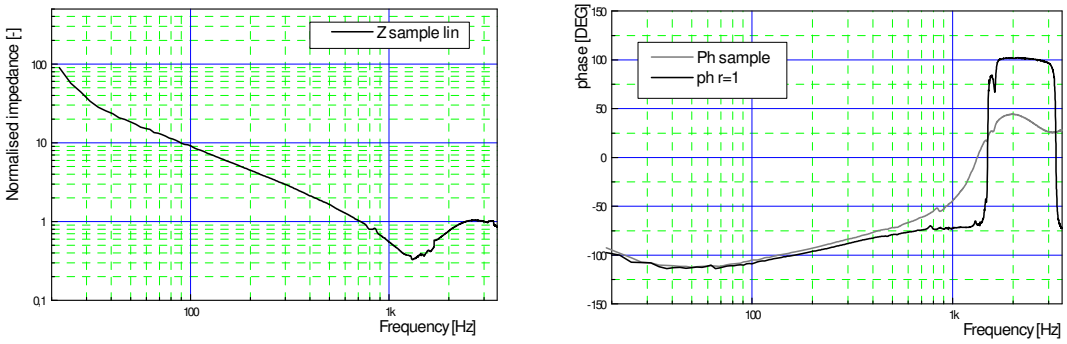

Fig. 6.12 (left): Normalized impedance at the position of the pu probe an absorbing sample at the end. Fig. 6.13 (right): Phase response in the tube. Black line: rigid termination, grey line: with an acoustic sample at the end.

The phase response of the pu probe in the standing wave tube is shown in Fig. 6.13. The black line shows the phase response of the pu probe with a rigid termination, the grey line shows the response when the absorbing sample is mounted at the end of the tube.

First the phase response of the pu probe is determined as if the probe is used in the free field. The free field phase response is obtained by correcting the measured phase response in the impedance tube with the phase of the known standing wave in the tube. In the rigidly closed tube the phase of the sound field is ±90 degrees so in order to get the free field response, 90 degrees is added for frequencies up to f_p. This is the frequency of the pressure minimum (at 1494Hz) and this is also the frequency where the tube response flips from -90degrees to 90 degrees. In the frequency range from f_p to f_u (the velocity minimum at 3263Hz), 90 degrees is subtracted. At frequencies higher than f_u, 90 degrees is added again. The phase response is not smooth around the frequencies f_p and f_u. Therefore, at these frequencies the phase is kept constant to get a better estimation. The result is shown in Fig. 6.14.

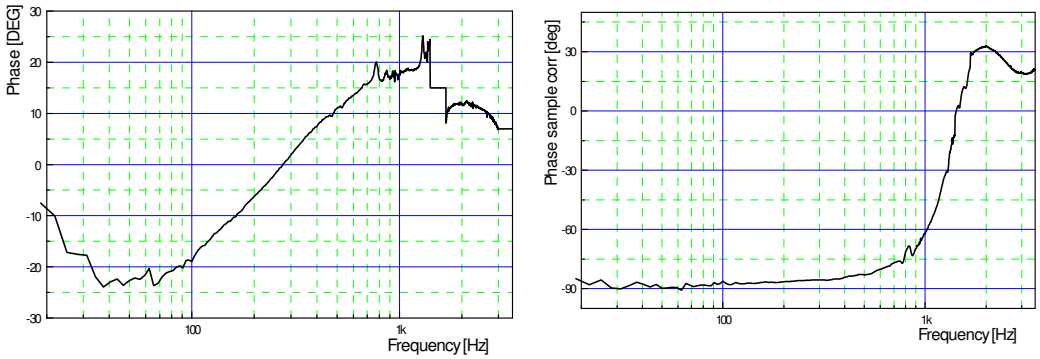

Fig. 6.14 (left): Corrected free field phase response of a pu probe. At the flipping' frequencies the response is obtained by interpolation. Fig. 6.15 (right): The corrected phase response of the acoustic sample in the tube.

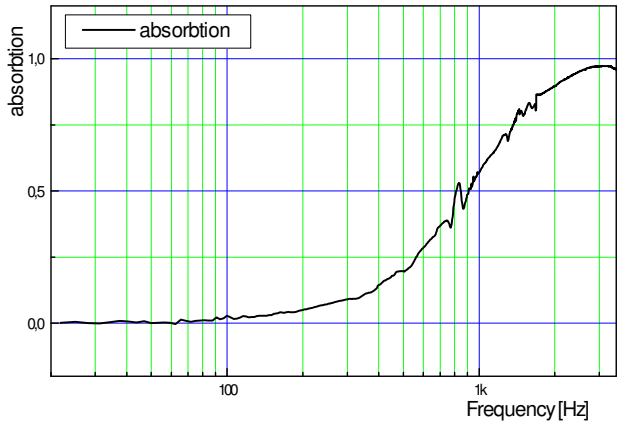

Fig. 6.16: Absorption coefficient measured in the Kundt's tube.

The 'free field' phase response (the phase response measured in a tube but corrected for the tube's behaviour, Fig. 6.14) is used to correct the phase response of the absorbing sample in the tube (Fig. 6.14, grey line): see Fig. 6.15.

Now the modulus (Fig. 6.12) and the phase response (Fig. 6.15) of the impedance due to the acoustic sample are known, the absorption coefficient can be calculated with Eq. (6.7), see Fig. 6.16.

Relation between impedance and reflection coefficient

As shown above, the reflection coefficient is given by the ratio of the outward travelling pressure wave and the incoming travelling pressure wave (Eq. (6.2) and Eq. (6.3)).

$$\left.\begin{aligned} p_{in}(x) &= p_0\ e^{ikx} \\ p_{out}(x) &= p_0\ R(\omega)e^{-ikx} \end{aligned}\right\} \rightarrow \frac{p_{out}(x)}{p_{in}(x)} = \frac{p_0\ R(\omega)e^{-ikx}}{p_0\ e^{ikx}} = R(\omega)e^{-2ikx} \qquad (6.16)$$

The inward and sound waves cannot be measured directly with a pressure microphone or a Microflown.

The sound waves are plane in the tube and the sound pressure and the particle velocity that can be measured at a certain position are given by:

$$\begin{aligned} p_{tot}(x) &= p_{out}(x) + p_{in}(x) = p_0 \left(e^{ikx} + R(\omega)e^{-ikx}\right) \\ u_{tot}(x) &= \frac{1}{\rho_0}\int \frac{\partial p_{tot}(x)}{\partial x}dt = \frac{p_0}{\rho_0 c}\left(e^{ikx} - R(\omega)e^{-ikx}\right) \end{aligned} \tag{6.17}$$

If the sensitivity of the velocity probe is adjusted so that $S = \rho_0 c$ then:

$$\begin{aligned} p_{tot}(x) - Su_{tot}(x) &= p_0 \left\{\left(e^{ikx} + R(\omega)e^{-ikx}\right) - \frac{S}{\rho_0 c}\left(e^{ikx} - R(\omega)e^{-ikx}\right)\right\} \\ &= p_0 \left\{\left(e^{ikx} + R(\omega)e^{-ikx}\right) - \left(e^{ikx} - R(\omega)e^{-ikx}\right)\right\} \\ &= p_0 2R(\omega)e^{-ikx} \end{aligned} \tag{6.18}$$

$$\begin{aligned} p_{tot}(x) + Su_{tot}(x) &= p_0 \left\{\left(e^{ikx} + R(\omega)e^{-ikx}\right) + \left(e^{ikx} - R(\omega)e^{-ikx}\right)\right\} \\ &= p_0 2e^{ikx} \end{aligned}$$

The ratio of the sum and the difference signal is given by:

$$\frac{p_{tot}(x) - Su_{tot}(x)}{p_{tot}(x) + Su_{tot}(x)} = \frac{p_0 2R(\omega)e^{-ikx}}{p_0 2e^{ikx}} = R(\omega)e^{-2ikx} = \frac{p_{out}(x)}{p_{in}(x)} \tag{6.19}$$

This makes sense because the sum signal of pressure and velocity gives an assembly that has a cardioid directivity. That is a directivity that has (in one dimension, i.e. the tube) a zero sensitivity in one direction and a double sensitivity in the other.

The latter can be rewritten to Eq. (6.7):

$$R(\omega)e^{-2ikx} = \frac{p_{tot}(x) - Su_{tot}(x)}{p_{tot}(x) + Su_{tot}(x)} = \frac{\frac{p_{tot}(x)}{u_{tot}(x)} - \rho_0 c}{\frac{p_{tot}(x)}{u_{tot}(x)} + \rho_0 c} = \frac{Z(x) - \rho_0 c}{Z(x) + \rho_0 c} \tag{6.20}$$

6.5. Surface impedance technique

Free field methods are important because the tube methods can be not accurate. The acoustic properties of materials can alter when they are put in a tube [30], [31], [32]. The tube measurements are destructive (a sample has to be cut) and only the normal reflection coefficient can determined in a limited bandwidth.

Fig. 6.17: Free field setup can be used inside a car.

The surface impedance technique is an in situ method to determine the reflection coefficient of acoustic material. The acoustic impedance is measure close to an acoustic material and the reflection coefficient is derived from that.

The method allows the reflection coefficient to be measured broad banded and also under an angle. The reflection coefficient of highly reflective materials are difficult to measure at lower frequencies.

Image source model with plane wave reflection coefficient

The image source model with plane wave reflection coefficient model is relatively straightforward.

The sound pressure and particle velocity field from a point source is given by (see also chapter 9: 'Monopole sound sources'):

$$p(r) = i\rho ck\frac{Q}{4\pi r}e^{-ikr} \;\; ; \;\; u(r) = \frac{Q}{4\pi}\frac{ikr+1}{r^2}e^{-ikr} \tag{6.21}$$

The impedance in the free field is therefore given by:

$$Z_{ff} = \frac{p(h_s - h)}{u(h_s - h)} = \frac{i\rho ck \frac{Q}{4\pi(h_s - h)} e^{-ik(h_s - h)}}{\frac{Q}{4\pi} \frac{ik(h_s - h)+1}{(h_s - h)^2} e^{-ik(h_s - h)}} = \frac{ik(h_s - h)}{ik(h_s - h)+1} \rho c \tag{6.22}$$

With Q the source strength, *k* the wavenumber, h_s the distance from the point source to the sample and *h* the distance from the impedance probe to the sample.

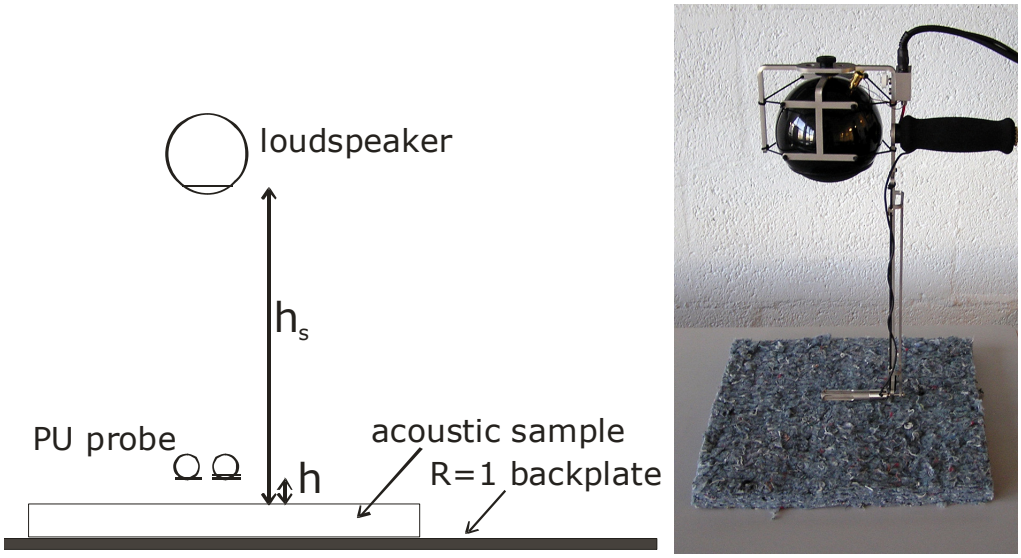

Fig. 6.18: Free field setup.

The impedance close to an acoustic sample is given by:

$$\begin{aligned} Z_{measure} &= \frac{i\rho ck \frac{Q}{4\pi(h_s - h)} e^{-ik(h_s - h)} + i\rho ck \frac{Q}{4\pi(h_s + h)} e^{-ik(h_s + h)} R}{\frac{Q}{4\pi} \frac{ik(h_s - h)+1}{(h_s - h)^2} e^{-ik(h_s - h)} - R \frac{Q}{4\pi} \frac{ik(h_s + h)+1}{(h_s + h)^2} e^{-ik(h_s + h)}} \\ &= \frac{\frac{e^{-ik(h_s - h)}}{(h_s - h)} + R \frac{e^{-ik(h_s + h)}}{(h_s + h)}}{\left(\frac{ik(h_s - h)+1}{ik(h_s - h)}\right) \frac{e^{-ik(h_s - h)}}{(h_s - h)} - R \left(\frac{ik(h_s + h)+1}{ik(h_s + h)}\right) \frac{e^{-ik(h_s + h)}}{(h_s + h)}} \rho c \end{aligned} \tag{6.23}$$

The ratio of the measurement impedance and the free field impedance is:

$$\frac{Z_{measure}}{Z_{ff}} = \frac{\frac{e^{-ik(h_s - h)}}{(h_s - h)} + R \frac{e^{-ik(h_s + h)}}{(h_s + h)}}{\frac{e^{-ik(h_s - h)}}{(h_s - h)} - R \left(\frac{ik(h_s - h)}{ik(h_s - h)+1}\right) \left(\frac{ik(h_s + h)+1}{ik(h_s + h)}\right) \frac{e^{-ik(h_s + h)}}{(h_s + h)}} \tag{6.24}$$

With that the reflection coefficient can be derived:

$$R = \frac{\frac{Z_{measure}}{Z_{ff}} - 1}{\frac{Z_{measure}}{Z_{ff}} \left(\frac{h_s - h}{h_s + h} \right) \left(\frac{ik(h_s + h) + 1}{ik(h_s - h) + 1} \right) + 1} \frac{h_s + h}{h_s - h} e^{ik\,2h} \tag{6.25}$$

When the $Z_{measure}$ and Z_{ff} are measured close after each other, all amplifier settings, AD settings, calibration of the microphone and microphone etc. are likely to be unchanged. As long as this is true, the values do not have to known as they will vanish in the ratio $Z_{measure}/Z_{ff}$.

Eq. (6.25) is similar to the expressions shown in [6] and [29] but here it is shown more clear what the consequence of a fixed source-probe distance is. If Eq. (6.25) is observed for high frequencies (ikh_s>>1 -> f>>300Hz and h_s>>h), the equation simplifies to:

$$R = \frac{\frac{Z_{measure}}{Z_{ff}} - 1}{\frac{Z_{measure}}{Z_{ff}} + 1} e^{ik\,2h} \tag{6.26}$$

If h_s>>h, the equation is barely sensitive for the probe-sample distance h. So for higher frequencies (f>300Hz, for a source-probe distance of 18cm), the reflection coefficient is measured accurate. This is important to realize, especially in respect to the paragraph below: 'PU Kundt's tube vs. free field measurements'. In that paragraph it will be shown that for certain materials the Kundt's tube result is different than the free field measurements. The cause must be that the results in the Kundt's tube are wrong. This is something that is known in literature [30].

In [6] Eq. (6.25) is also derived for oblique angles. The end result is similar but the way it is derived is slightly different and therefore also shown here. Fig. 6.19 shows the setup for the measurement in the semi-anechoic room. Let θ be the angle of incidence, given by θ = arctan r/(h+d).

The incident wave which is travelling from the source to the probe is, at the position of the probe, given by:

$$p_{in} = \frac{p_0}{r_1} e^{i(\omega t + k r_1)} \tag{6.27}$$

with r_1 the distance between the source (S) and the probe. In this formula, d is the normal distance between the probe and the sample. To include the reflection of the sample, a mirror source (S') is placed behind the sample at the same distance as the physical source is placed from the sample.

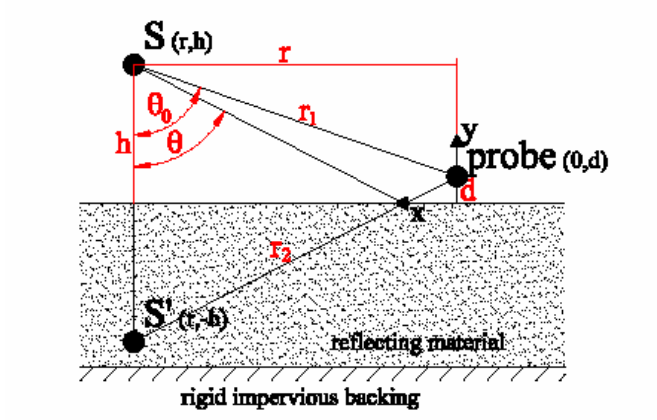

Fig. 6.19: Free field setup, oblique incidence (from [6]).

This assumption is only valid if the value kr_1 is sufficiently large [10]. The wave which is travelling from that mirror source in the direction of the probe is given by:

$$p_{out} = R(\omega,\theta)\frac{p_0}{r_2}\ e^{i(\omega t + kr_2)} \tag{6.28}$$

The total pressure at the position *(0,d)* is given by:

$$p_{tot} = p_{in} + p_{out} = p_0\left(\frac{e^{ikr_1}}{r_1} + R(\omega,\theta)\frac{e^{ikr_2}}{r_2}\right)e^{i\omega t} \tag{6.29}$$

The particle velocity, which is normal to the impedance plane, can now be deduced:

$$\begin{aligned} u_{tot} &= \frac{1}{\rho_0}\int\frac{\partial p_{tot}}{\partial x}dt \\ &= \frac{p_0}{\rho_0 c}\left(\frac{1-ikr_1}{-ikr_1}e^{ikr_1}\cos(\theta) - R(\omega,\theta)\frac{1-ikr_2}{-ikr_2}e^{ikr_2}\cos(\theta)\right)e^{i\omega t} \end{aligned} \tag{6.30}$$

The impedance at the position of the probe is given by:

$$Z(d,\omega) = \frac{p_{tot}(d,\omega)}{u_{tot}(d,\omega)} = \rho_0 c\frac{\frac{e^{ikr_1}}{r_1} + R(\omega,\theta)\frac{e^{ikr_2}}{r_2}}{\left(\frac{1-ikr_1}{-ikr_1}\right)e^{ikr_1}\cos\theta_0 - R(\omega,\theta)\left(\frac{1-ikr_2}{-ikr_2}\right)e^{ikr_2}\cos\theta} \tag{6.31}$$

The reflection coefficient of the absorbing surface can be deduced:

$$R(\omega,\theta) = e^{ik(r_1-r_2)}\frac{r_2}{r_1}\frac{Z(d,\omega)\left(\frac{1-ikr_1}{-ikr_1}\right)\cos\theta-\rho_0 c}{Z(d,\omega)\left(\frac{1-ikr_2}{-ikr_2}\right)\cos\theta_0+\rho_0 c} \tag{6.32}$$

If the pu probe is placed very close to the surface (d is very small), $\theta \approx \theta_0$ and $r_1 \approx r_2$. So, the expression simplifies:

$$R(\omega,\theta) = \frac{Z(d,\omega)\left(\frac{1-ikr_1}{-ikr_1}\right)\cos\theta-\rho_0 c}{Z(d,\omega)\left(\frac{1-ikr_2}{-ikr_2}\right)\cos\theta+\rho_0 c} \tag{6.33}$$

Since the mirror-source-model is only valid if kr_1 is sufficiently large, the expression simplifies to:

$$R(\omega,\theta) = \frac{Z\cos\theta-\rho_0 c}{Z\cos\theta+\rho_0 c} \tag{6.34}$$

If the same 'trick' is used as is described in Eq. (6.25), that is taking the ratio of the measured surface impedance $Z_{measured}$ and the free field impedance Z_{ff}, then the cosine theta factor does not have to be used.

The pu-probe is rotated to the desired angle and calibrated in this orientation. Then the sample is measured with the pu-probe normal to the surface. Eq. (6.25) can then be used to calculate the reflection coefficient from the measured values.

Moving average filtering

Below a measurement is shown of a calibration in a normal room and (red line) and the signal that was time windowed to remove the room reflections (black line). As can be seen, the black line follows the red line and is found in the middle. Many measurements have been done and this effect was always found.

Therefore a function 'moving average' was tested and found to have similar results. A calibration measurement was done in an anechoic room and repeated in a normal room to show this.

As can be seen in Fig. 6.20: , the calibration result in an anechoic room is a smooth line with some small ripples. The result in a normal room seems to be 'noisy'. This 'noisy' signal is not because of a poor signal to noise ratio but due to the room reflections.

Because the room reflections have a random character, i.e. the reflections are from all possible directions with all possible phase shifts, the deviation from the anechoic calibration is also random. As long as the

deviations are random (and thus the reflections are random), the moving average method will work.

At lower frequencies (f<150Hz) the method seems to break up and this is most probably caused by a dominant reflection (e.g. the ground reflection). For frequencies lower than 80Hz the method does not work, most probable due to the relative high background sound pressure levels).

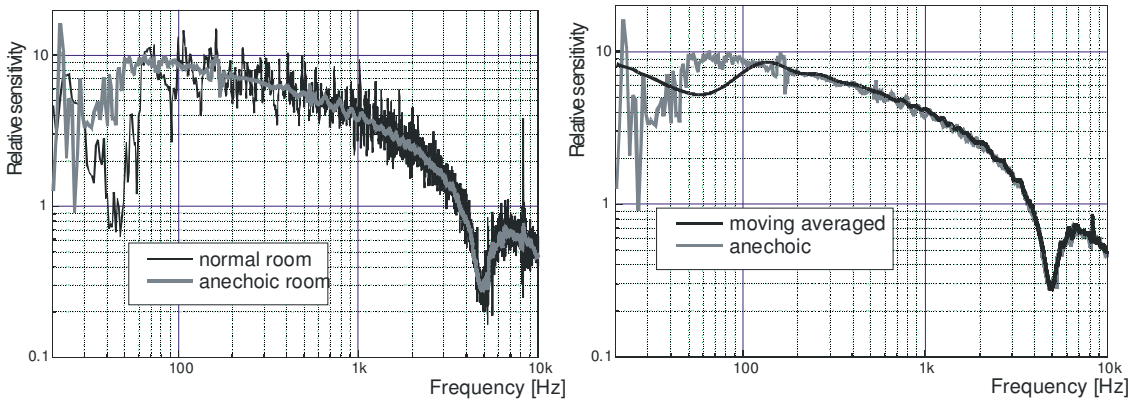

Fig. 6.20: A calibration measurement in an anechoic room (grey line) and in a normal room (black line). Right: same measurement in an anechoic room (grey line). Black line is the moving averaged result of the calibration measurement in a normal room that was shown in the left plot.

Surface impedance technique comparison with Tamura method

Measurements in the semi-anechoic room were executed on the same test as was used in the Kundt's tube, see paragraph 6.4. An absorbing sample surface of 2.2m^2 was used and the measurement time to obtain the absorption coefficient for a certain incidence angle was less than 10 minutes for the chosen frequency range [6].

First, a measurement of the impedance at normal sound incidence was performed. The source was placed at different heights above the pu-probe, which was placed directly on the absorbing surface. So, the distance between the sample and the Microflown and microphone was approx. 6mm.

The results of these measurements, together with a simulation are presented in Fig. 6.21.

Next to the measurements with the pu probe and the simulation based on the theoretical model, a curve is shown that is deduced from a Tamura measurement on a sample surface of approx. 10m^2. A measurement time of 4 hours is needed to deduce the absorption coefficient for all incidence angles in the chosen frequency range (200Hz-8kHz).

There's a good correspondence between the results of both measurement techniques.

The vertical distance probe-source was kept 76cm and the probe was moved over the absorbing surface. The results for an angle of 60^o are shown in Fig. 6.21. As expected, these measurements are, at higher frequencies,

influenced by noise. The results of the Tamura [26], [27] measurement are also shown in both figures.

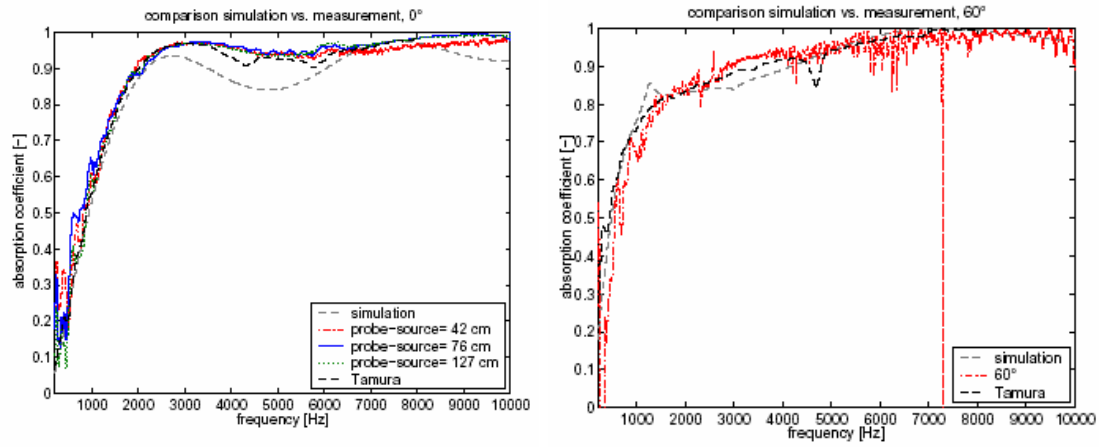

Fig. 6.21: Free field setup, (left) normal incidence, (right) oblique (60°) incidence, from [6].

The results of these measurements, together with a simulation are presented in Fig. 6.21.

Next to the measurements with the pu probe and the simulation based on the theoretical model, a curve is shown that is deduced from a Tamura measurement on a sample surface of approx. $10m^2$. A measurement time of 4 hours is needed to deduce the absorption coefficient for all incidence angles in the chosen frequency range (200Hz-8kHz).

There's a good correspondence between the results of both measurement techniques.

The vertical distance probe-source was kept 76cm and the probe was moved over the absorbing surface. The results for an angle of 60° are shown in Fig. 6.21. As expected, these measurements are, at higher frequencies, influenced by noise. The results of the Tamura [26], [27] measurement are also shown in both figures.

The advantages of the measurement with a pu probe compared to the Tamura technique are the smaller sample size, the smaller measurement time and the simpler mathematics.

Another advantage is the fact that out of the measurement at a certain position the absorption coefficient for that incidence angle can be deduced. The Tamura technique needs a measurement at all angles before one can deduce the absorption coefficient for a certain incidence angle.

PU Kundt's tube vs. surface impedance technique

Five materials are measured in a Kundt's tube. The material properties are first measured in a Kundt's tube and then compared with the free field method. This paragraph is a summary of [31], [32].

A: 25mm Foamex
B: 25mm Foamex with reflective foil
C: 25mm Akotherm (white) D20/25 polyester wool 0.5kg/m^2
D: 25mm Acusticab: 30 kg/m^3 polyurethane foam with 0,025mm polyurethane film on top. At the back is a thin adhesive layer.
E: 1.2kg/m^2 felt that is used for automotive applications

		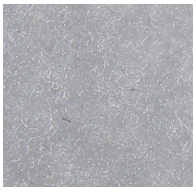	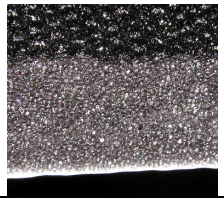	
A: Foamex I	B: Foamex II	C: Akotherm	D: Acusticab	E: felt

The acoustic field in the tube is measured with a PU probe. First the probe is calibrated in the tube by measuring the response of the PU probe without an acoustic sample of the fully reflective end of the closed tube, see paragraph 6.4. Then a sample is inserted, the impedance is measured and the reflection and absorption coefficient is calculated.

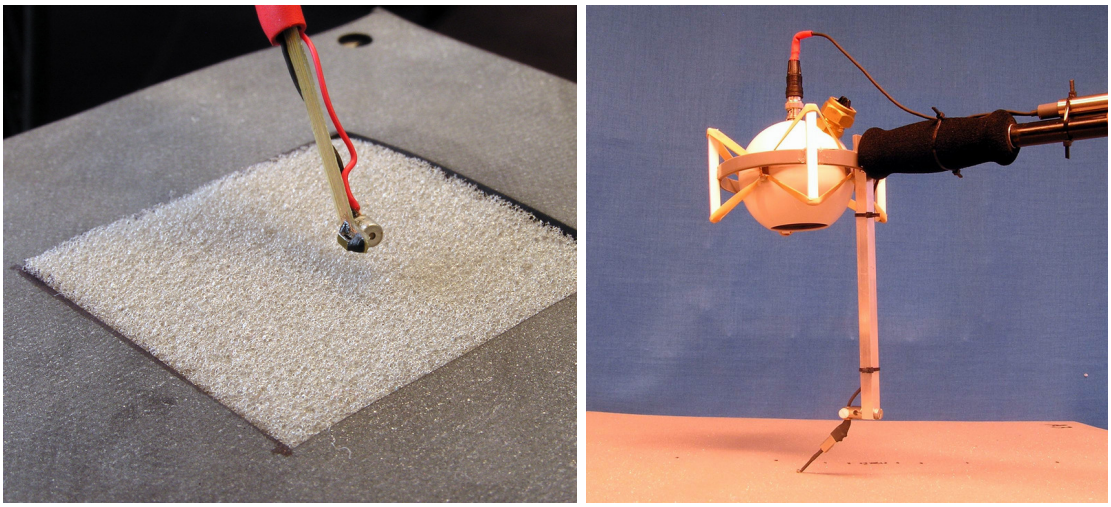

Fig. 6.22: Left: the acoustic samples are mounted in the tube and measured with the free field method with a PU match. Right: a large sample is measured.

After this, the free field absorption coefficient is measured and compared with the Kundt's tube results. The red lines in Fig. 6.22 show the free field response when the sample is still mounted in the tube (see Fig. 6.22, left) and the blue lines show the free field response of a 60cmx60cm sample (see Fig. 6.22, right).

As can be seen, the Kundt's tube result matches the free field response if the sample is mounted in the tube. However the free field response of a large sample does not always match the response of a small sample mounted in a tube.

It can therefore be concluded that the acoustic properties change if a sample is cut and put in a tube.

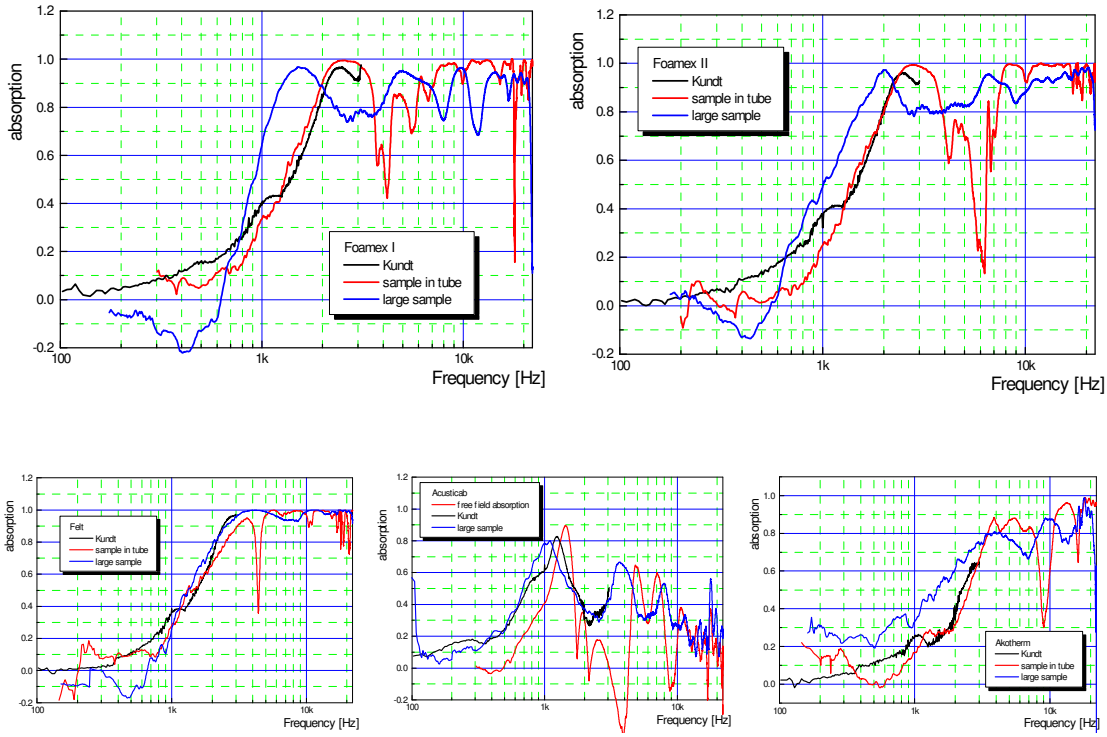

Fig. 6.23: The acoustic samples are mounted in the tube and measured with a PU Kundt's tube (black line); with the free field method (PU match) and the sample still mounted in the tube (red line); and a large sample in the free field (blue line).

The changing of the acoustic properties is made even more clear in [32]. In an experiment the sample size was changed from 15cmx15cm to 1cmx1cm. Simple wooden structures are used as boundary to simulate the Kundt's tube mounting, see Fig. 6.24 (left).

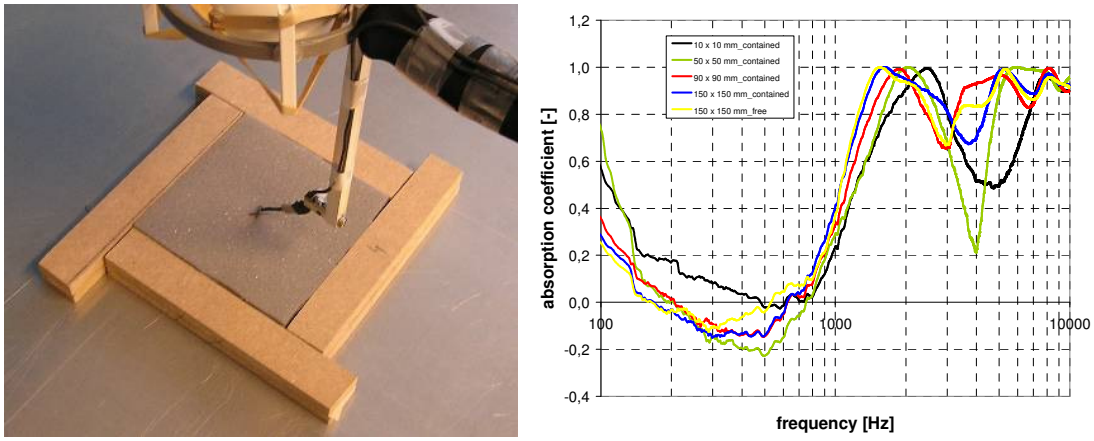

Fig. 6.24 (left): a sample is contained with a wooden border to simulate the Kundt's tube mounting. Right: The measurement results of various sample sizes.

As can be seen in Fig. 6.24 right, the absorption changes if the sample size changes. For a larger sample size, free field response coincides with a contained response. This indicates that for this material the tube diameter should be larger than 15cm. This however would mean that the upper usable frequency of the tube is in the order of 1kHz, this is well below the interesting bandwidth.

Measurements at DAF Trucks / Paccar

At DAF Trucks (a Paccar company) preliminary tests were done to evaluate impedance measurements with a pu sensor. The final goal is to be able to measure acoustic properties of materials applied in the interior of truck cabins. The pu sensor was calibrated as explained above and two types of foam were measured at several angles, see Fig. 6.25.

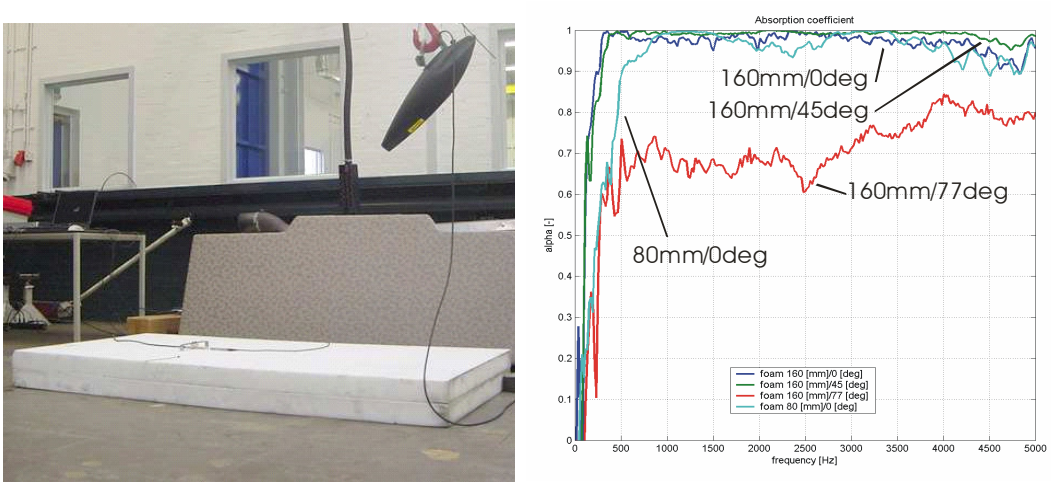

Fig. 6.25 (Left): Free field setup. Right: Absorption measurements for different material thicknesses and angle of incidence.

The behaviour of the foam is quite according to expectation: very high absorption above a critical frequency. This critical frequency depends on the thickness of the foam layer; 160mm foam absorbs well above 300Hz ($\approx 0.14\lambda$) and a layer of 80mm foam performs well above 500-800Hz ($\approx 0.1\lambda$-0.2λ).

In this experiment for 77° angle of incidence the resulting alpha value is not as expected; because the normal particle velocity is very small the measurements suffer from bad signal to noise ratio. It is expected that this is due to the fact that not enough sound power was used to drive the speaker and the distance between speaker and sensor was too large.

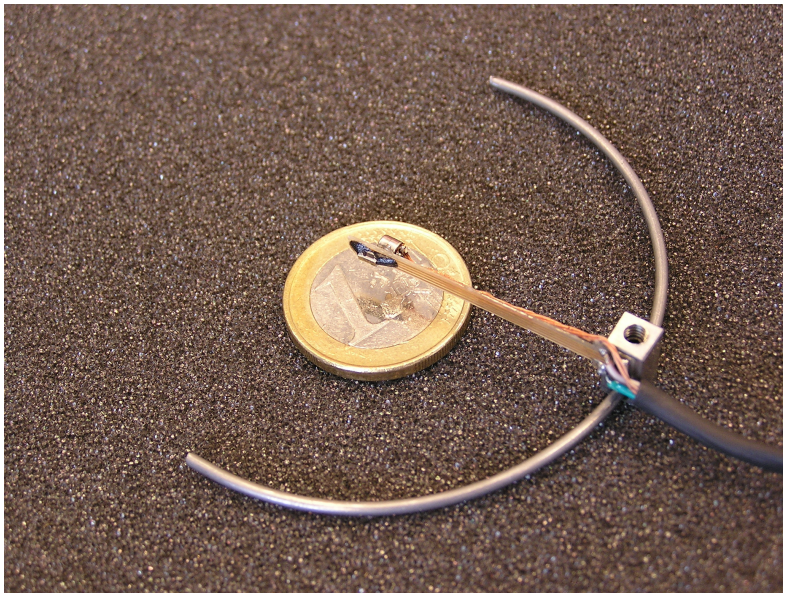

Fig. 6.26: PU match also used for surface impedance measurements.

Surface impedance technique, F-term correction

The plane wave model is valid as long as the source is 'far' from the measurement surface. This is not very practical, especially at lower frequencies.

The following method to convert the spherical reflection coefficient to a planar one. The method is tested and it is good, but it takes a lot of effort and time to get it working. Once working the method is time consuming (several minutes to process) and the mathematics are so complex that it is difficult to understand.

The F-term is used for the transformation of the spherical reflection coefficient to the planar reflection coefficient. The transformation is proposed in 1985 by Nobile and Hayek [8]. Later the model of the initial surface impedance method [6] was improved with this F-term [7].

Spherical waves are reflected in a different way than plane waves. For locally reacting surfaces it can be shown that the following approximate relation exists:

$$R_s = R_p + (1 - R_p) F(\omega) \tag{6.35}$$

R_p is the reflection coefficient for plane waves and R_s is the reflection coefficient for spherical waves.

The *F*-term is an important term in this solution. However, this term cannot be calculated directly because the *F*-term depends on the plane wave reflection coefficient R_p, which is not known beforehand. So, the reflection coefficient R_p has to be calculated in an iterative way.

Some MATLAB scripts use a simple optimization strategy to find the plane wave reflection coefficient and surface impedance from the measured

impedance obtained with a point source above a reflecting surface. The measured impedance is thus the spherical wave impedance.

An initial guess for β (the normalized admittance $=1/Z_p$) has to be made: e.g. $\beta=10+10i$. The plane wave reflection coefficient is then calculated by:

$$R_p = \frac{\sin(\theta)-\beta}{\sin(\theta)+\beta} \tag{6.36}$$

The parameter θ is the angle (=90DEG for normal incidence).

Now, the *F*-term can be calculated based on the initial guess:

$$F(\omega) = 1 + i\sqrt{\pi}\lambda \mathrm{e}^{-\lambda^2}\, erfc(-i\lambda) \tag{6.37}$$

$$\lambda = \sqrt{ikr_2}\sqrt{1+\beta\sin(\theta)-\sqrt{1-\beta^2}\cos(\theta)} \tag{6.38}$$

K is the wave number, r_1 is distance source – probe and r_2 is distance mirror source – probe. *Erfc*(*x*) is the complementary error function defined as:

$$erfc(x) = \frac{2}{\sqrt{\pi}}\int_x^\infty e^{-t^2}dt = 1-\frac{2}{\sqrt{\pi}}\int_0^x e^{-t^2}dt \tag{6.39}$$

Now an estimation of the spherical wave reflection coefficient R_s and the spherical wave impedance Z_s can be made:

$$R_s = R_p + (1-R_p)F(\omega) \tag{6.40}$$

The impedance Z_s, the pressure *p* and the velocity *u* are obtained from the acoustic potential:

$$\phi = \frac{e^{ikr_1}}{r_1} + R_s\frac{e^{ikr_2}}{r_2} \quad ; \quad p = -i\omega\rho\phi \quad ; \quad u = grad(\phi) \quad ; \quad Z_s = \frac{p}{u} \tag{6.41}$$

This is an estimate, therefore the calculated spherical wave impedance is not equal to the measured spherical wave impedance. The error is defined as:

$$\text{Error} = |Z_s - Z_{measured}| \tag{6.42}$$

The error is minimized by varying the impedance in an optimization procedure (the default Nelder-Mead simplex method is used). The best estimate for the plane wave reflection coefficient is found, when the error has a minimum.

The optimization procedure starts at the highest frequency. When a solution is found, this solution is used as the initial value for the next frequency. The optimization procedure is stopped when the maximum number of function evaluations is reached or when the optimum value is found (the changes in succeeding function evaluations are smaller than a given tolerance).

Surface impedance technique, low frequencies

At low frequencies the source is relatively close to the measurement surface and therefore the sound waves are becoming more spherical. One can correct for this with the F-term correction however this model expects a point source. The sound power that is emitted by a point source however is proportional with the frequency squared, indicating that such a source is not an efficient radiator at low frequencies. See also chapter 9: 'monopole sound source'.

So for low frequencies the source radiation properties have an influence on the measurement and to correct for this, one is restricted to a point source that does not emit sound pressure at low frequencies.

Acoustic damping materials normally have a low absorption at low frequencies and the surface impedance method has difficulties at such conditions. This is because a low particle velocity due to a high reflection coefficient, a low pressure because a point source emits a low sound pressure field at low frequencies and there is usually a relative high level of background noise at low frequencies.

The low frequency monopole that is described in chapter 9 paragraph 9.7, has a very high volume velocity output and with this source one is able to generate enough sound to be able to have sound pressure and particle velocity close to a fully reflecting plate and at low frequencies (30Hz is possible).

Surface impedance technique, signal to (background)noise level

The signal to noise ratio (S/N) of a measurement is an important figure. If it is too low, the measurement becomes not valid.

The signals of the sound pressure and the particle velocity are measured in the free field and close (4.5mm distance) to a fully reflective plane and with the source switched off and on. The (1W) loudspeaker was driven maximal with pink noise at 17cm distance. The signals might be better if a swept sine is applied.

Fig. 6.27 shows the responses. In the left plot the pressure responses are shown. As expected, the pressure response increases about 6dB due to the reflective plate. Below 100Hz the S/N drops below 10dB in the free field and close to the reflective plate the S/N is 6dB better.

The velocity signal has a much better S/N in the free field. Below 100Hz the S/N drops below 40dB. However when the probe is positioned very close to the reflective plane the S/N drops below 15dB.

Conclusion is that for lower frequencies the S/N of the sound pressure signal becomes low due to the monopole radiation behaviour and if the probe is positioned close to a reflective plane the S/N of the particle velocity is low due to the reflection.

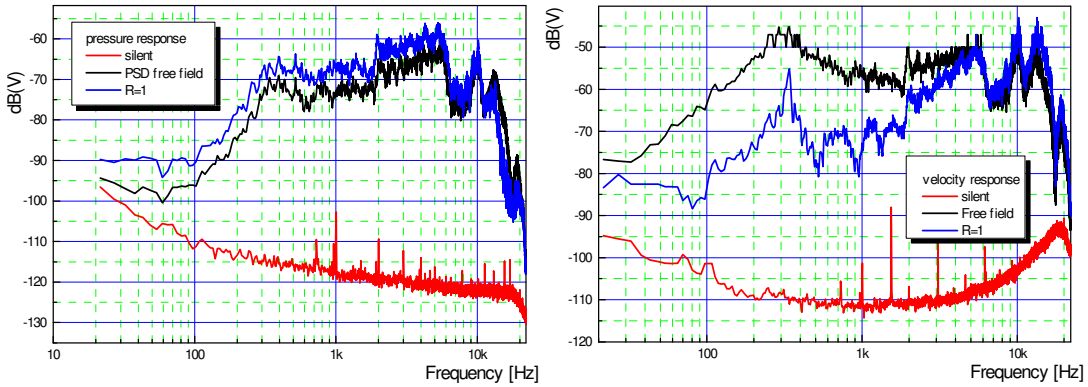

Fig. 6.27 (left): Pressure signals and (right): velocity signals (PU match). Red lines: silent response, blue lines: pink noise on the loudspeaker and close to fully reflective plate, black lines: free field response to pink noise.

Measurement of a plane with R=1

The measurement of a fully reflective plane is the most difficult scenario for this method. This is because the particle velocity level is low close to a fully reflective plane (see also paragraph below: 'Signal to (background)noise level'). Apart from that, the measurement is very sensitive for phase errors. The only thing that is simple about a fully reflective plane is that the spherical reflection coefficient equals the planar reflection coefficient. The model that is used here is therefore valid.

In the measurement (at 4.5mm distance) of the impedance of the (80cmx80cm) reflective plane a ripple occurs. This ripple is caused by standing waves between the reflective plane and the loudspeaker. The ripples can be removed by the moving average algorithm. It is our believe that a larger source-sample distance can reduce this effect. This is a point of further R&D.

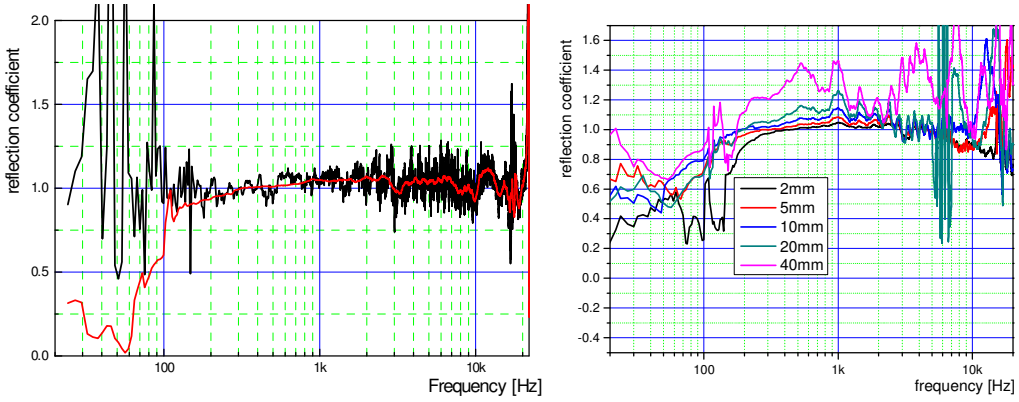

Fig. 6.28 (left): A measurement result of a 80cmx80cm fully reflective plate (measurement distance h: 4.5mm 18cm source-sample). Black line without moving average smoothing red line: with moving averaging smoothing. Right: An 80cmx80cm fully reflective plate measured at several probe-sample distances (source-sample distance: 18cm).

A small monopole sound source is also tried. The monopole source is not used because the frequency response shows a high dynamic range (which makes measurements difficult at frequencies with a low sound emission) and this type of source makes the setup less portable.

The measurement of a fully reflective plate shows within what limits the method works in worst case conditions. As can be seen in Fig. 6.28 (red line), the error is relatively small in a frequency range from 200Hz up to 15kHz. Tests show that the ripples in the response are caused by a standing wave between the loudspeaker and the fully reflective plate.

The black line shows the measured reflection coefficient when the signals are not smoothed. All room reflections (in both calibration and measurement) are present and the effect of the standing wave between the reflective plate and the loudspeaker is not filtered.

It can expected that the measurement error will drop considerable if the material becomes less reflective.

The fully reflective plate can therefore be used as estimate for the maximal measurement error. In this example the measurement (Fig. 6.28) error is in the order of 5% in a 200Hz-6kHz bandwidth for a 18cm source-sample distance.

Fig. 6.28 Right shows the results of measurements with several probe-sample distances (source-sample distance: 18cm). As can be seen: The accuracy of the 2mm probe-sample distance is low for frequencies lower than 200Hz. This is caused by a poor signal to noise ratio. Measurements between 5mm and 10mm show good results.

Surface impedance technique, influence of measurement distance

In this paragraph the effect of the measurement distance is shown. First a measurement of Foamex 1 is measured at 2mm and 10mm. Then in the software the distance *h*, is varied in 1mm steps around the real measurement distance.

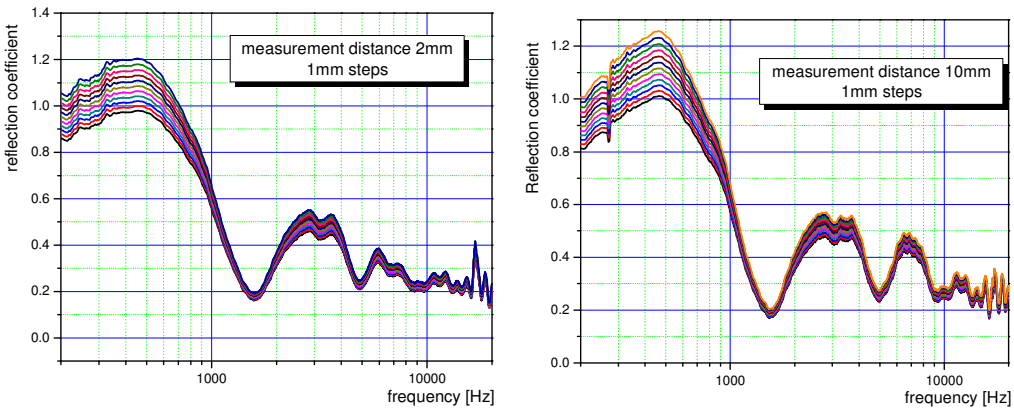

Fig. 6.29 (left): Foamex 1 measured at 2mm and the absorption is calculated for a variation of measurement distances (from -3mm to 7mm). Right: the measurement distance is 10mm and results are calculated from 4mm to 15mm. The middle line is the proper distance.

The 2mm distance is varied in the software from -3mm to +7mm. The result is shown in Fig. 6.29, left. As can be seen: the influence is most when the reflection coefficient is high.

Same shows for the same material measured at 10mm. If the absorption is calculated for a distance varied from 4mm to 15mm, the results are influenced when the reflection coefficient is high.

A large sample of Foamex 1 is measured at several measurement distances. These distances are also used for the processing. The results are shown in Fig. 6.30. As can be seen, the measurements in a range from 2mm up to 20mm are consistent and when the distance is increased further, the results deviate.

The measurement results have a reflection coefficient higher than 1 which is obviously wrong. Why this error occurs is not clear.

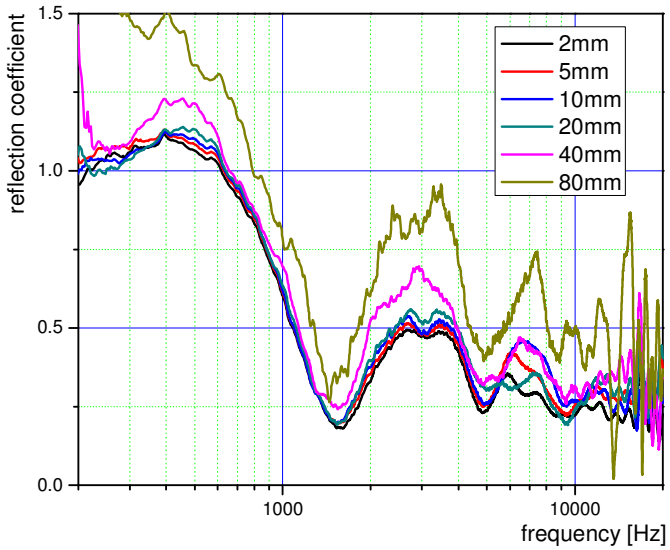

Fig. 6.30 : Foamex 1 measured at several distances.

Surface impedance technique, influence of environment

For this test 25mm Foamex is used and two source-sample distances are used: 17cm and 32cm. To check the influence of the acoustic environment several measurements where done:

a) a large sample of 60cmx60cm was measured as reference
b) a 30cmx30cm sample that was cut free
c) a smaller (15cmx15cm) sample that was cut free
d) a very small (4.5cmx4.5cm) sample that was cut free
e) a very small (4.5cmx4.5cm) sample put in the end of a kundt's tube (see Fig. 6.22)
f) 60cmx60cm sample two reflective vertical planes (see, Fig. 6.31, left)
g) 60cmx60cm two reflective horizontal planes (see, Fig. 6.31, right)

In Fig. 6.32 the influence of several environments is shown.

The black line shows the response measured close (3mm) to the large reference sample. The green line, that almost overlaps, is the response if two horizontal planes are put over the acoustic material with 8cm from the probe, see Fig. 6.31 (right). It can be concluded that horizontal reflective planes do not influence the measurement much.

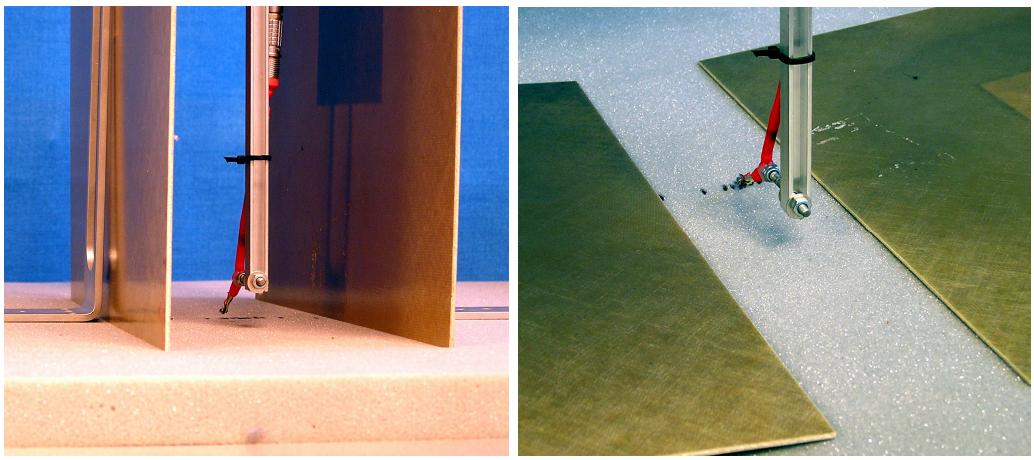

Fig. 6.31 (left): two vertical reflective planes, (right): two horizontal reflective planes.

If the sample is cut to 15cmx15cm the response is similar except for a 'dip' around 2500Hz, see Fig. 6.32 red line. See further 'sample size' below.

If the free field conditions are disturbed with two vertical planes 6cm from the probe, see Fig. 6.31 (left), the response will alter in to the blue line. It can be concluded that vertical obstacles do not influence the measurement much.

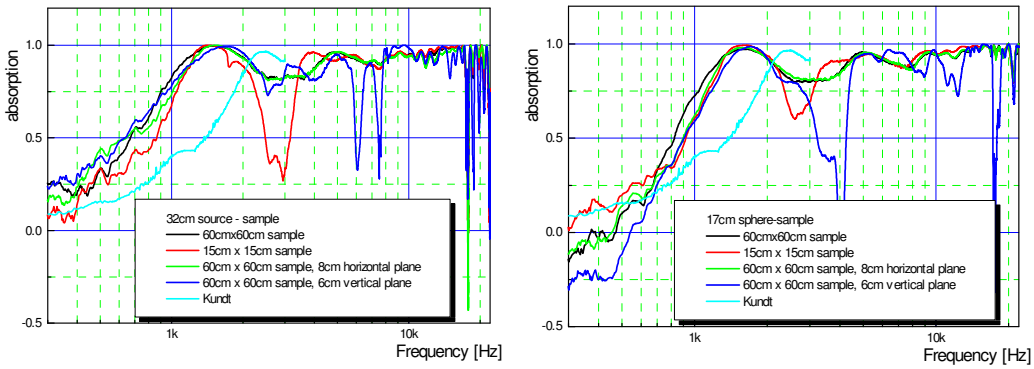

Fig. 6.32: Influence of acoustic environment. Black: large reference sample, red: smaller sample cut free; dark blue: with two horizontal reflective planes as shown in Fig. 6.31 (right).

For comparison the kundt's tube measurement is shown in yellow. It can be concluded that if the sample is cut and put in the tube, the properties of the material change: the maximal absorption is shifted from 1800Hz to 2500Hz.

Surface impedance technique, influence of sample size

In Fig. 6.33 the influence of the sample size is shown. The reference 60cmx60cm sample is shown in light blue. If the sample size is reduced to 15cmx15cm, a deviation of the response is seen at 2500Hz (dark blue line). More deviations are seen if the size is reduced to 15cmx15cm and the deviation seen at 2500Hz increases (green line).

If the size is reduced to 4.5cmx4.5cm, the complete shape alters: the maximal absorption increases in frequency. This effect is observed if the sample is free (red line) and, (black line) contained in a kundt's tube holder (as shown in Fig. 6.22). The small sample shows similarity with a measurement in a Kundt's tube (purple line).

It can be concluded that the sample size is influencing the measurement. However it is most probable that the acoustic properties of the sample change and that the free field measurement is valid.

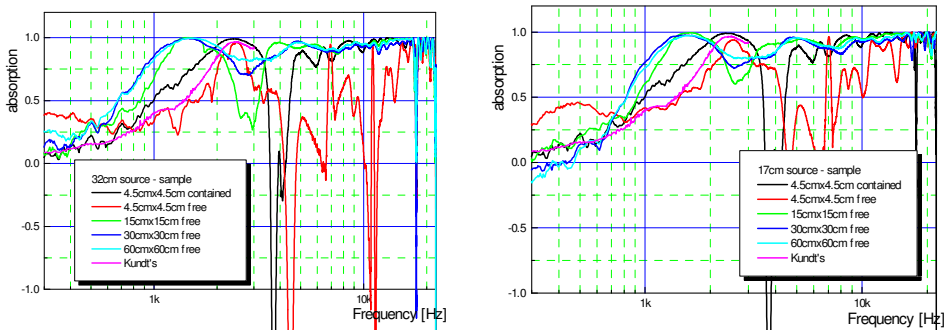

Fig. 6.33: Influence of sample size. Left: source sample distance 32cm, right the distance is 17cm.

Surface impedance technique, influence of horizontal obstacles

Two reflective horizontal plates are put on the 60cmx60cm reference sample to check what their influence is, see Fig. 6.31 (right). As can be seen in the graph below (Fig. 6.34), if the reflective planes are 8cm away from the probe that the response is not affected.

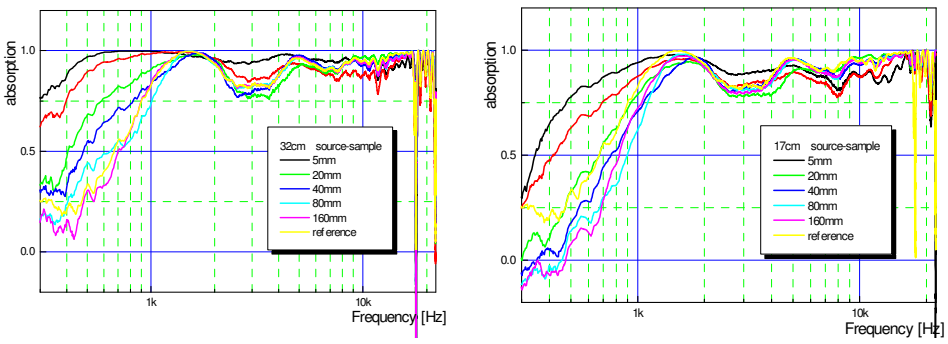

Fig. 6.34: Influence of horizontal reflective planes. Left: source sample distance 32cm, right the distance is 17cm.

Surface impedance technique, influence of vertical obstacles

Two reflective vertical plates are put on the 60cmx60cm reference sample to check what the influence is, see Fig. 6.31 (left). As can be seen in the graph below (Fig. 6.35), if the reflective planes are 6cm away from the probe that the response is not affected much.

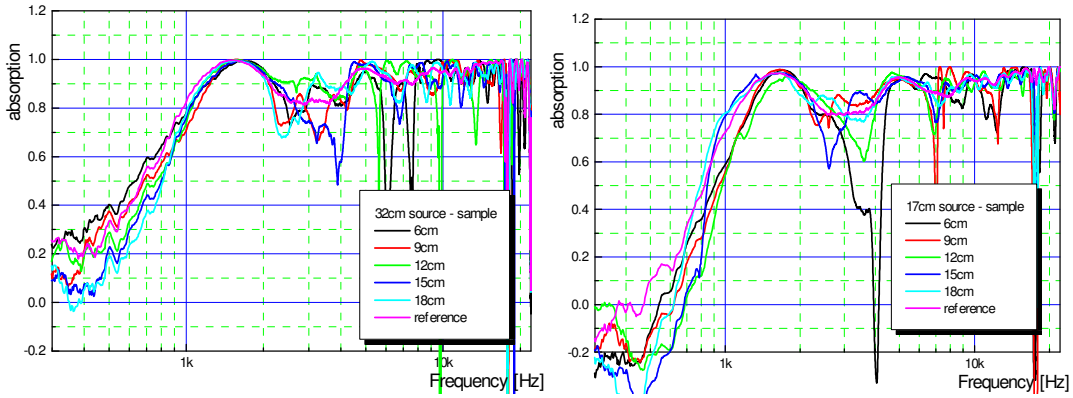

Fig. 6.35: Influence of vertical reflective planes. Left: source sample distance 32cm, right the distance is 17cm.

Stability over the time

The absorption coefficient measured over the eight days time period for small contained and large PU foam is shown below. For both samples, there is natural scatter of absorption coefficient observed at frequencies below 800 Hz for small contained and below 650 Hz for large sample. Also, the values of absorption coefficient are negative below these frequencies. In case of small contained foam, there is scatter at higher frequencies above 3000 Hz observed too. This scatter is not characteristic for a large sample. The reflections from the rigid walls of the container can be responsible for the scatter of the absorption coefficient for small sample at higher frequencies.

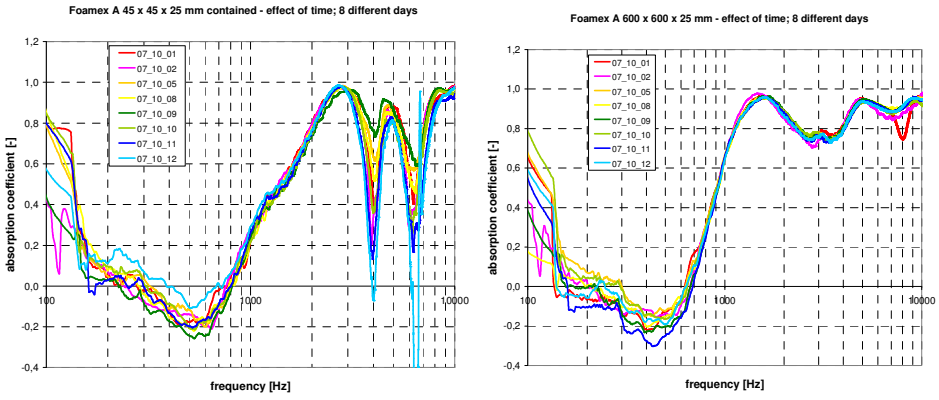

Fig. 6.36: Stability over time.

Reproducibility

To find out the reproducibility the absorption of the same sample was measured several times.

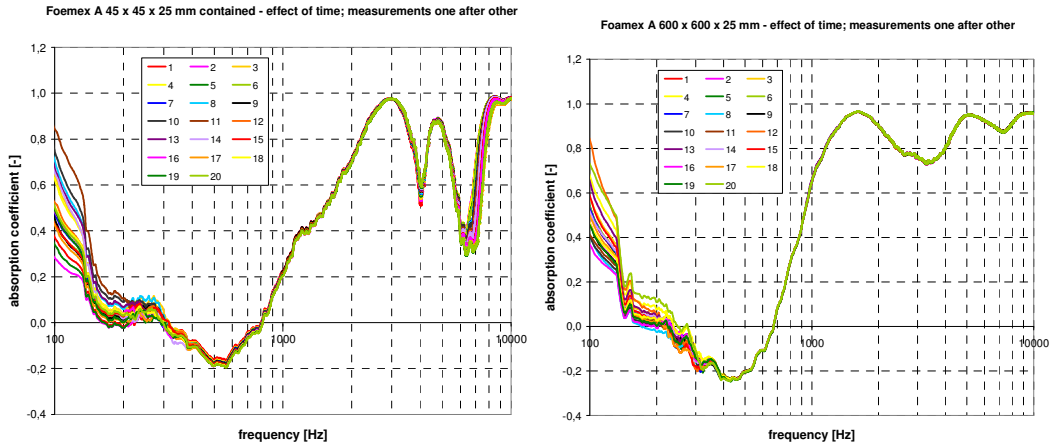

Fig. 6.37: Reproducibility measurement.

As can be seen, the measurement result does not change much for frequencies higher than 300Hz. This indicates that the method is stable for frequencies higher than 300Hz. For lower frequencies the methods shows some deviations. This may be caused by the low signal to noise ratio of the method at these low frequencies. See also the paragraph 'signal to (background)noise level' some pages back.

Effect of different operator

To show the robustness of the method several persons were asked to do a calibration and measurement. These persons did not have any experience with the method or with acoustic measurements in general. As can be seen, the results do not deviate much for frequencies higher than 500Hz. This indicates also that if measurements are done with more care, the quality increases at lower frequencies.

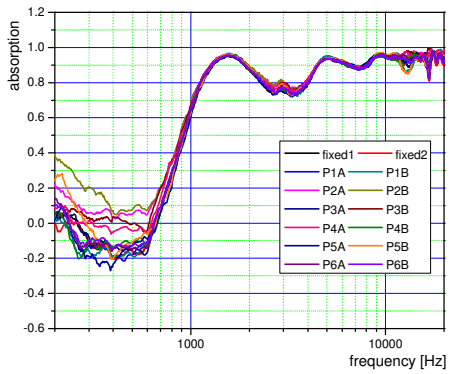

Fig. 6.38: Effect of different operator.

Effect of background noises and reverberant surrounding

The effect of different background noise and reverberant surrounding is presented below.

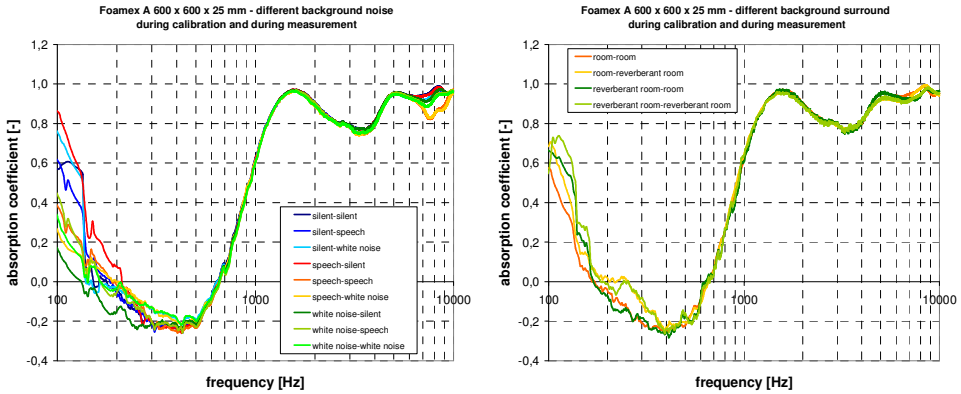

Fig. 6.39: Effect background noise and acoustic environment.

The absorption coefficient measurement of the measured sample is not affected by background noises (applied during calibration and measurement) above 400Hz. The free-field surface impedance method can be used in the reverberant environment (car, reverberant room, etc…) or in the noisy surrounding (assembling hall, offices, etc.…) without affecting the result much.

Effect of ambient temperature change

The absorption of a test sample is measured in a car and the temperature in the car was increased from 10°C to 30°C. The measurement result that is presented on the left shows the absorption when the setup was calibrated (inside the car) and measuring at several temperatures.

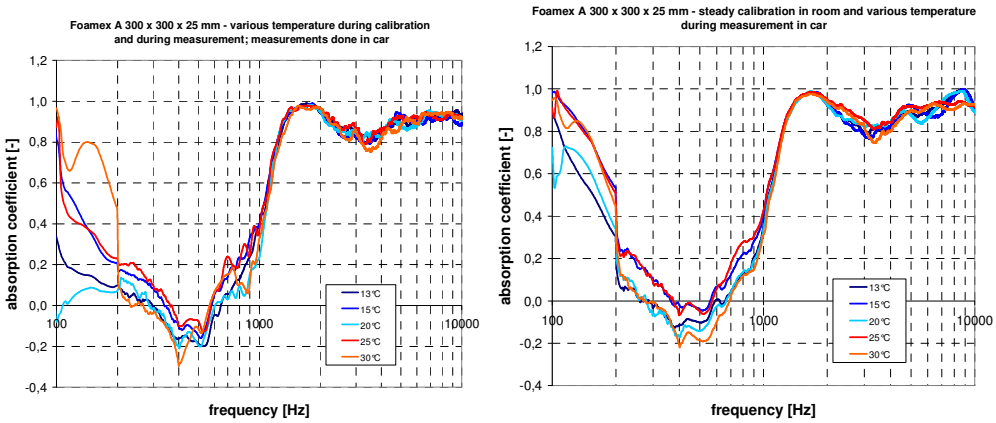

Fig. 6.40: Effect of temperature change.

The measurement result that is presented on the right shows the absorption when the setup was calibrated once at 10°C (inside the car) and measuring at several temperatures.

This observation shows that the hand-held free-field measurement device which is used to measure the acoustic impedance of the material can be used in certain temperature range without significant influence to absorption coefficient of the measured material.

Measurement with wind / moving surface [34], [35]

Measurements are done in the presence of wind or when the probe is moving. The wind measurements are shown in chapter 12: 'DC flow, Protection & Windshields'. The other measurements are shown below.

A 95mm diameter patch of "cotton felt" is mounted on a rotated disk with increasing speed. A standard measurement set up is positioned at 15cm from the surface the absorption coefficient is measured and compared relative to the still standing sample. If the measurement time is reduced errors in the FFT calculation occur starting at lower frequencies. It shows it is still possible to determine the absorption with reasonable accuracy using standard non parametric transfer function estimation if an area of constant surface impedance is measured for more than 0.05 seconds. Driving on a highway at 80km/h this means the resolution of this method would be 1.1 meter. At 0.04 seconds errors occur at lower frequencies. Results at even shorter time periods might be achieved in the future with dedicated parametric estimation methods.

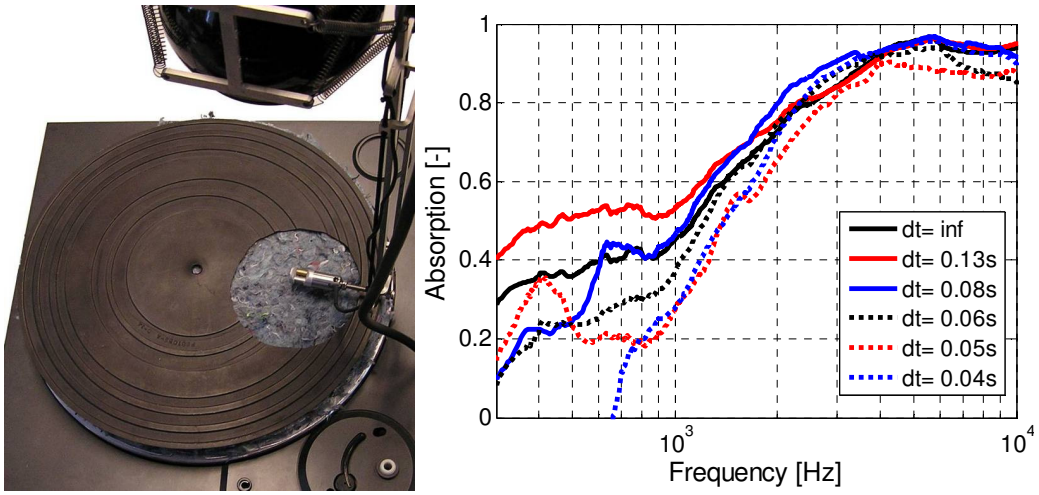

Fig. 6.41: Absorption of a movingsample.

Measurements under an angle

In the previous theory the measured impedance must be corrected with a cosine of the measurement angle. However if the same 'trick' is used as is described in Eq. (6.25), that is taking the ratio of the measured surface

impedance $Z_{measured}$ and the free field impedance Z_{ff}, then the cosine theta factor does not have to be used.

The pu-probe is rotated to the desired angle and calibrated in this orientation. Then the sample is measured with the pu-probe normal to the surface. Eq. (6.25) can then be used to calculate the reflection coefficient from the measured values.

At lower frequencies the measurements clearly deviate from real values as they are negative. The coherence however is high from 200Hz upwards. At higher frequencies (f>1kHz) the measured values are more realistic. No explanation is found for the low frequency deviation yet.

If a material is locally reacting, the acoustic properties are *not* changing with measurement angle. In most cases materials are believed to be locally reacting (this makes live easy because one has only to measure the absorption under one angle). In practice however it shows that almost all materials are locally reacting, in other words their acoustic properties change if the angle of incidence changes.

The Foamex material is measured under several angles and it shows that the absorption is changing for changing measurement angles.

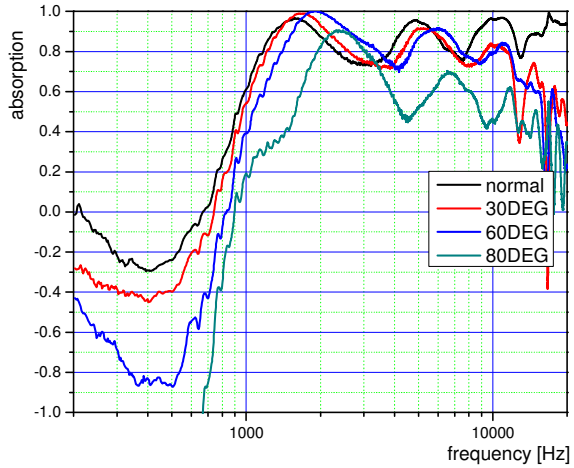

Fig. 6.42: Measurements with a normal and oblique angle.

Measurement errors

The method shows to be sensitive for materials with a high reflection coefficient and especially at lower frequencies the results have a higher error.

1) In general the reason for these errors can be found in:
2) wrong model
3) bad signal to noise ratio
4) wrong measurement distance
5) wrong source behaviour
6) wrong calibration

7) properties of the acoustic sample
8) sample size

1) The model does not explain the measurement error: the measurement on a fully reflective plate has a higher accuracy than a measurement of Foamex. 2) The measurements on a fully reflective plate show also that the signal to noise ratio is not the cause of this error; the measurement error is consistent.

3) If the probe sample distance is underestimated (so if at 1cm distance is measured but 7mm is used for the model), the measurements results resemble better the tube results. The physical reason for this under estimation (if any) is unknown.

4) The model that is used here assumes a loudspeaker with a monopole behaviour. The real loudspeaker does have a behaviour that only resembles a monopole. If the source-probe measurement distance increases to 30cm or more the behaviour deviates less than 0.05dB and 1.5Degree from a true monopole source. Increasing the source-probe distance to 30cm must improve the measurement if the deviation in behaviour at close distances is the cause of the inaccuracy.

5) Errors in the calibration can be expected at lower frequencies. The moving average is a source of errors in the lower frequencies. However, the problems occur also at higher frequencies and these problems cannot be explained with a wrong calibration.

6) A negative absorption can be a local effect. An average of the complete sample disproved this statement.

7) sample size or edge effects. If the sample is too small edge effects take place. This however is not causing the negative absorption values. A measurement with a larger sample did not solve the issue.

The properties of the acoustic sample can be the reason for the measurement error.

Measurements in a car

A sample of 15cmx15cm Foamex 1 is prepared with a reflective plate behind it to be used as a piece of material with known properties. This sample is now placed in several positions in a car with the doors open and closed.

Fig. 6.43: Measurements of a test sample at several positions in a car.

As can be seen below, the measurement results are consistent and not influenced by an open or closed door. The foot area seems a difficult place to measure: the results deviate at lower frequencies.

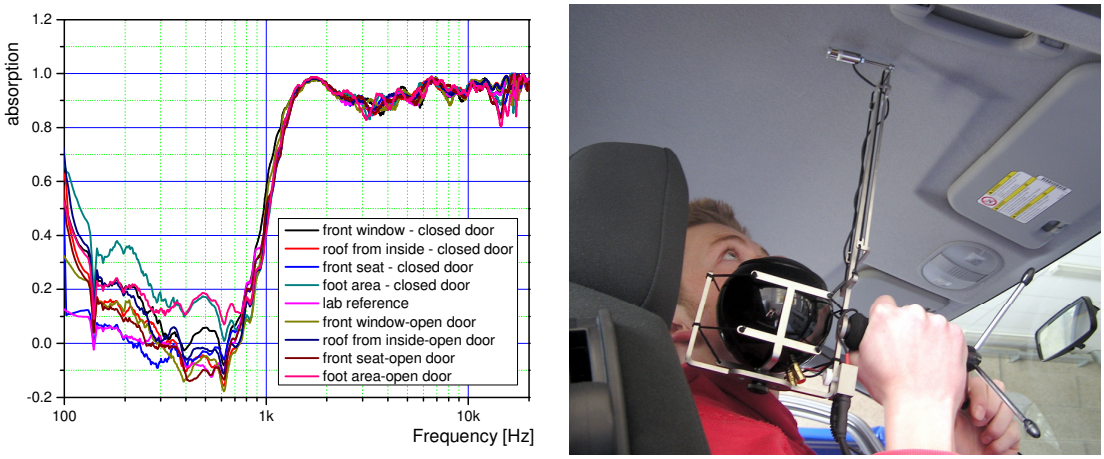

Fig. 6.44: Measurement results of a test sample at several positions in a car.

Headliner and seat measurements

In a measurement campaign the headliners and passenger seats of 25 cars of the same make are investigated to find out if the acoustic properties are similar after assembly.

The measurements are taken with a mobile setup. The required 152 measurements are taken in only 2 hours of total measuring time (including the walking around between the cars).

Headliner measurements

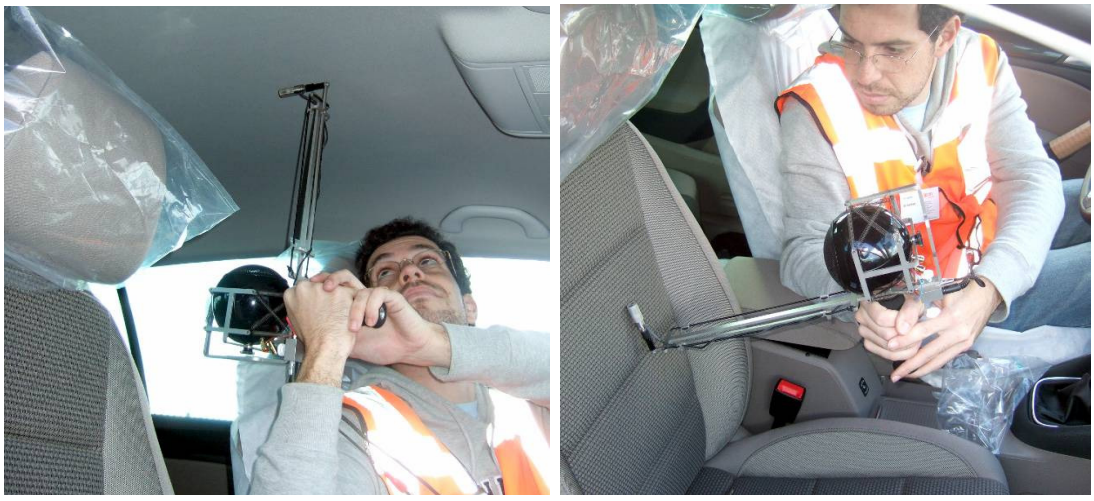

Fig. 6.45: In situ headliner and chair measurements.

In between the measurements of the 25 cars every time the reference car was measured. This gives an idea of the reproducibility of the method, see Fig. 6.55.

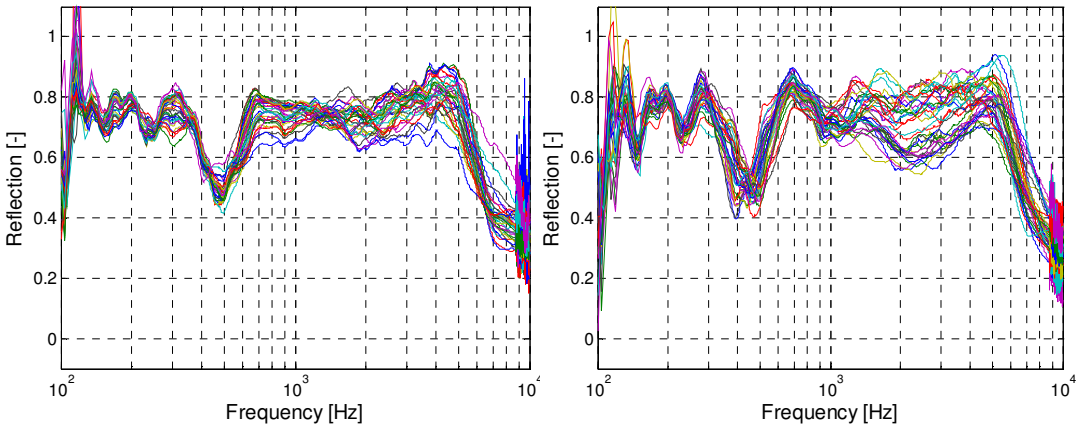

Fig. 6.46 (Left): 25 times the reflection coefficient of the headliner of the same car measured each time before a new car is measured.

Fig. 6.47 (Right): The reflection coefficient of the headliners of 25 different cars.

After the reference car, the headliner of a different car is measured. Those results are shown in Fig. 6.56. As can be seen, the deviation in the measurements of different cars is larger than the deviation in the reference cars indicating that the damping properties of the materials after assembly are not identical.

Seat measurements

In a similar way the reflection coefficient of the passenger seats next to the driver seat are measured. The measurement results are shown in Fig. 6.48.

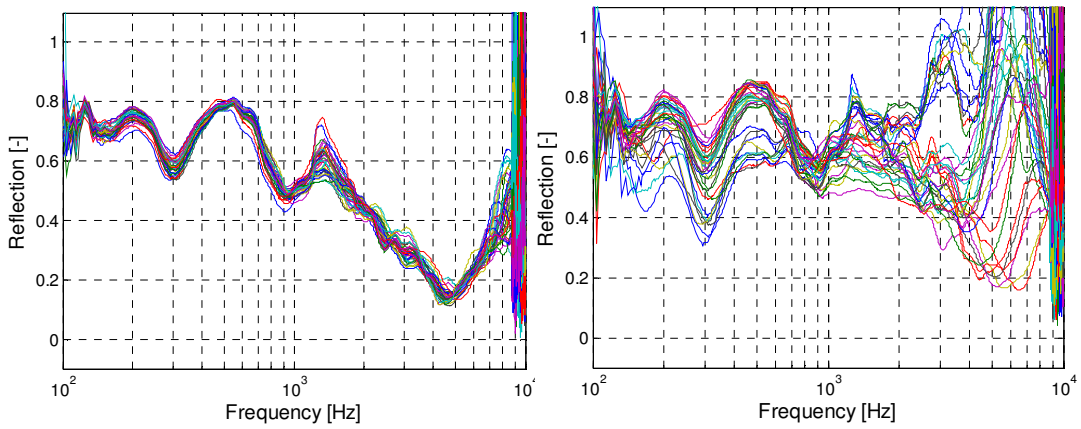

Fig. 6.48 (Left): 25 times the reflection coefficient of the seat of the same car measured each time before a new car is measured.

Fig. 6.49 (Right): The reflection coefficient of the seat of 25 different cars.

After each reference measurement a seat of a different car was measured. The variance of the test measurements is much larger than the variance in the reference measurements. This is a strong indication that the acoustic properties are very different for different seats, see Fig. 6.49.

variations over place

There is a slight variation in the measurements on the headliner of the reference car. This might be because it is difficult to measure on exactly the same position each time. The spatial variation of the reflection coefficient of the headliner is therefore investigated.

Variations over place of a headliner before mounting

First the variation of the reflection coefficient over space is measured of a typical headliner felt (not the same type as in the 25 cars). As can be seen in Fig. 6.50, the variance of the reflection coefficient in space is small for the felt measured in the laboratory.

The measurements show that there are spatial variations in the reflection coefficient across the headliner. These variations are caused by changes, suffered by the damping material, whilst being assembled in the car.

It has been also shown that the reflection coefficient of a single point in the headliner (or seat) is not representative of the whole headliner. In spite of the fact that the reflection coefficient (measured in the lab) of a typical headliner felt shows no spatial variation at all, this "no variation" assumption is not true for the mounted headliner.

Therefore, acoustic measurements inside the car after assembly are recommendable in order to investigate deviation and to have quality control. This data, taken at the end of the manufacturing process, can also be used to feed acoustic models created to calculate the sound field inside the car.

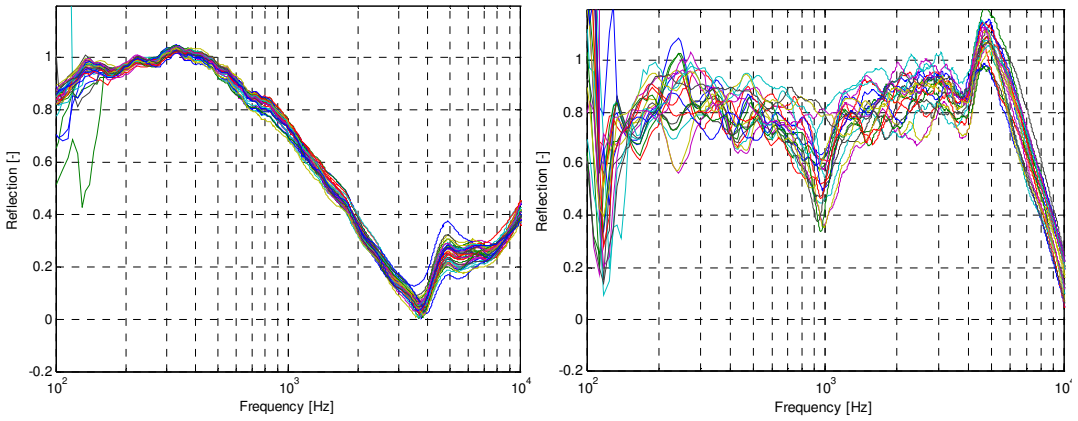

Fig. 6.50 (Left): 25 times the reflection coefficient of a typical headliner felt before mounting at different positions.

Fig. 6.51 (Right): 25 times the reflection coefficient of the headliner of the same car in different positions

6.6. Measurement of inhomogeneous materials

This paragraph is a summary of [28]. The acoustic properties of some materials are likely to vary at each position. The properties of

inhomogeneous materials are measured with the surface impedance method. First results will be presented of local impedance measurements, giving a reflection coefficient at each position. These local measurements will be averaged over a surface and results will be compared with the PU Kundt's tube method that measures the average properties of a larger surface.

At lower frequencies the sound field becomes spherical and these results should be corrected with the PU surface impedance method. During this study these corrections are not applied since the frequency of interest is relative high.

Single quarter lambda resonator

A rigid plate with a single quarter lambda resonator is chosen to study a regional deviation of impedance, Fig. 6.52. A tube 62mm long with a 5.5mm diameter is mounted in a 115x115mm flat steel plate. This tube will predominantly absorb locally and only at one frequency when a quarter of the wave length equals the length of the tube (and at its higher harmonics). A miniature "PU match" probe is used to scan the surface and the inside of the resonator.

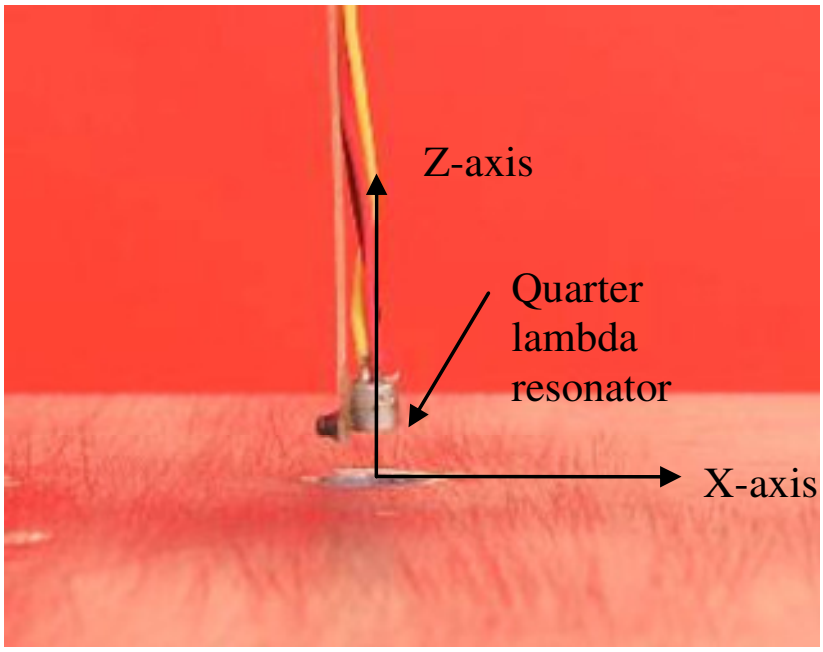

Fig. 6.52: PU match impedance probe sensitive in the direction of the Z-axis on a quarter lambda sample.

Movement over the surface (x-axis)

The probe is positioned 3mm above the plate and is moved from directly above the tube (x=0mm), along the plate. The results are plotted in Fig. 6.53 and Fig. 6.54. The autospectrum is not an absolute value but the deviation in decibels normalized with the free field calibration. A value of

0dB will represent a free field condition. Note that the impedance above the plate is mainly determined by particle velocity and pressure remains almost constant.

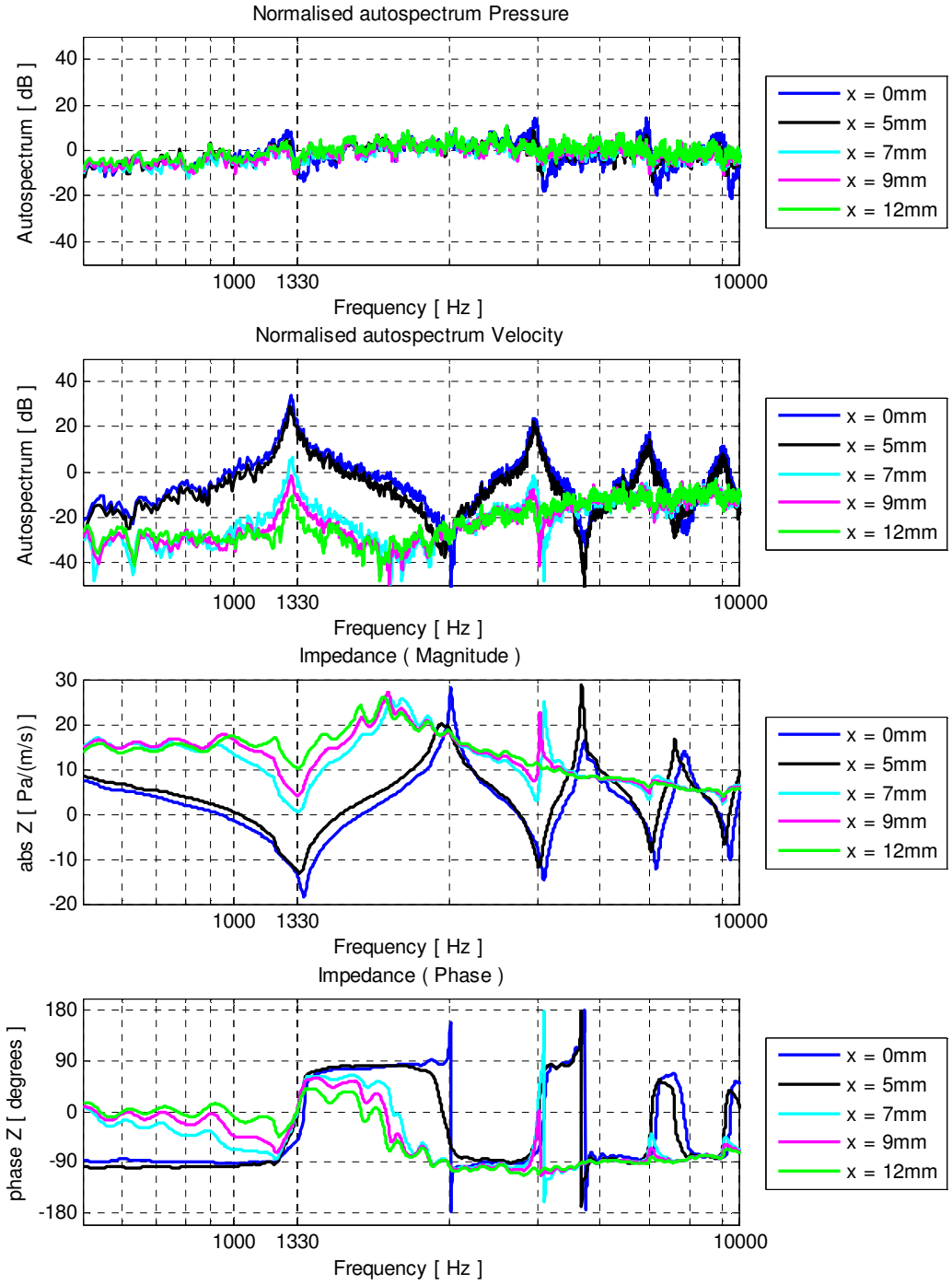

Fig. 6.53: Autospectrum and impedance at several locations 3mm from the surface.

In Fig. 6.54 an interesting phenomena can be observed at 1330Hz. The absorption equals 100% near the resonator (x=7mm), but directly above the resonator there is nearly 100% reflection (x=0mm). Since the imaginary part is zero at that frequency we are allowed to look only at the

real part. Above the tube the reflection is 1 but with negative phase, so -1. This is makes sense when is considered inside the tube nearly all energy is reflected. As the reflection or absorption coefficient is calculated the absolute value is taken and this information is lost.

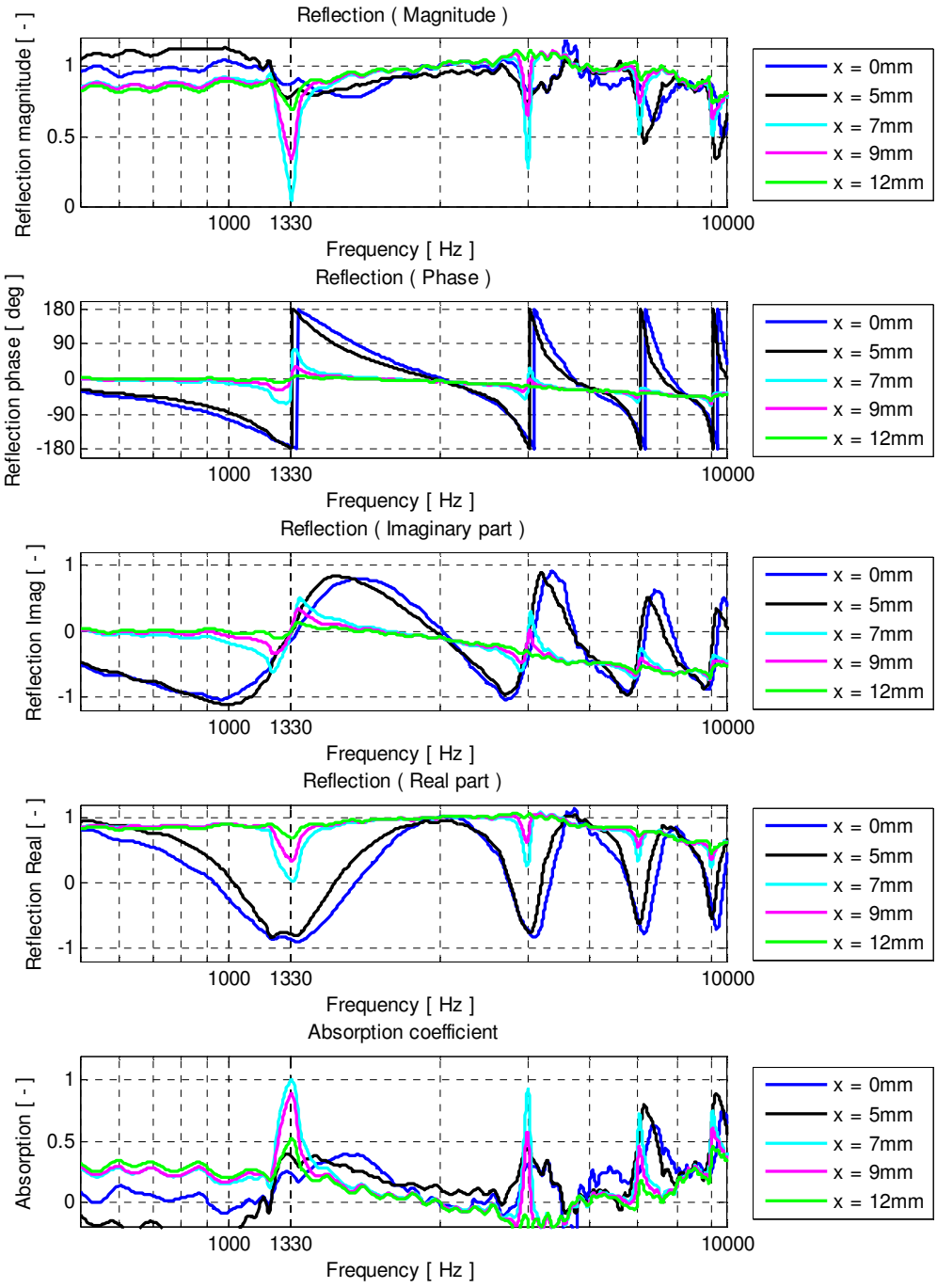

Fig. 6.54: Reflection and absorption at several locations 3mm from the surface.

Only directly above the tube the real part of the reflection could equal -1 at 1330 Hz. If a larger area would be covered a more averaged value unequal to -1 would be measured. This means the spatial resolution of this method must be in the order of millimeters.

Movement in the resonator (z-axis)

Next the probe is moved in the z direction from inside the tube (z=-14mm) to the surface of the plate (z=0 mm) and further to above the plate (z=6mm), see below.

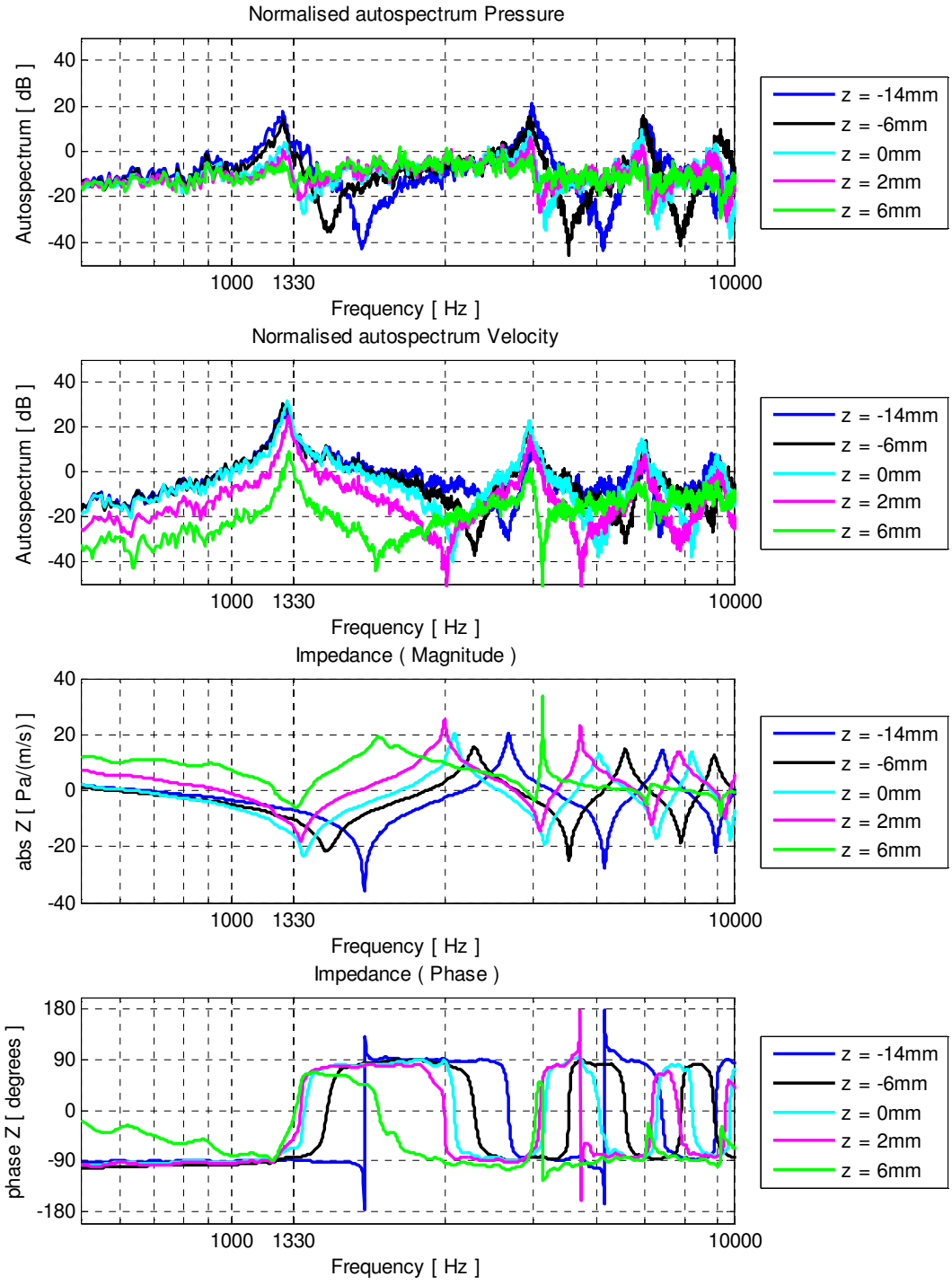

Fig. 6.55: Autospectrum and impedance along the z-axis (in and out the tube).

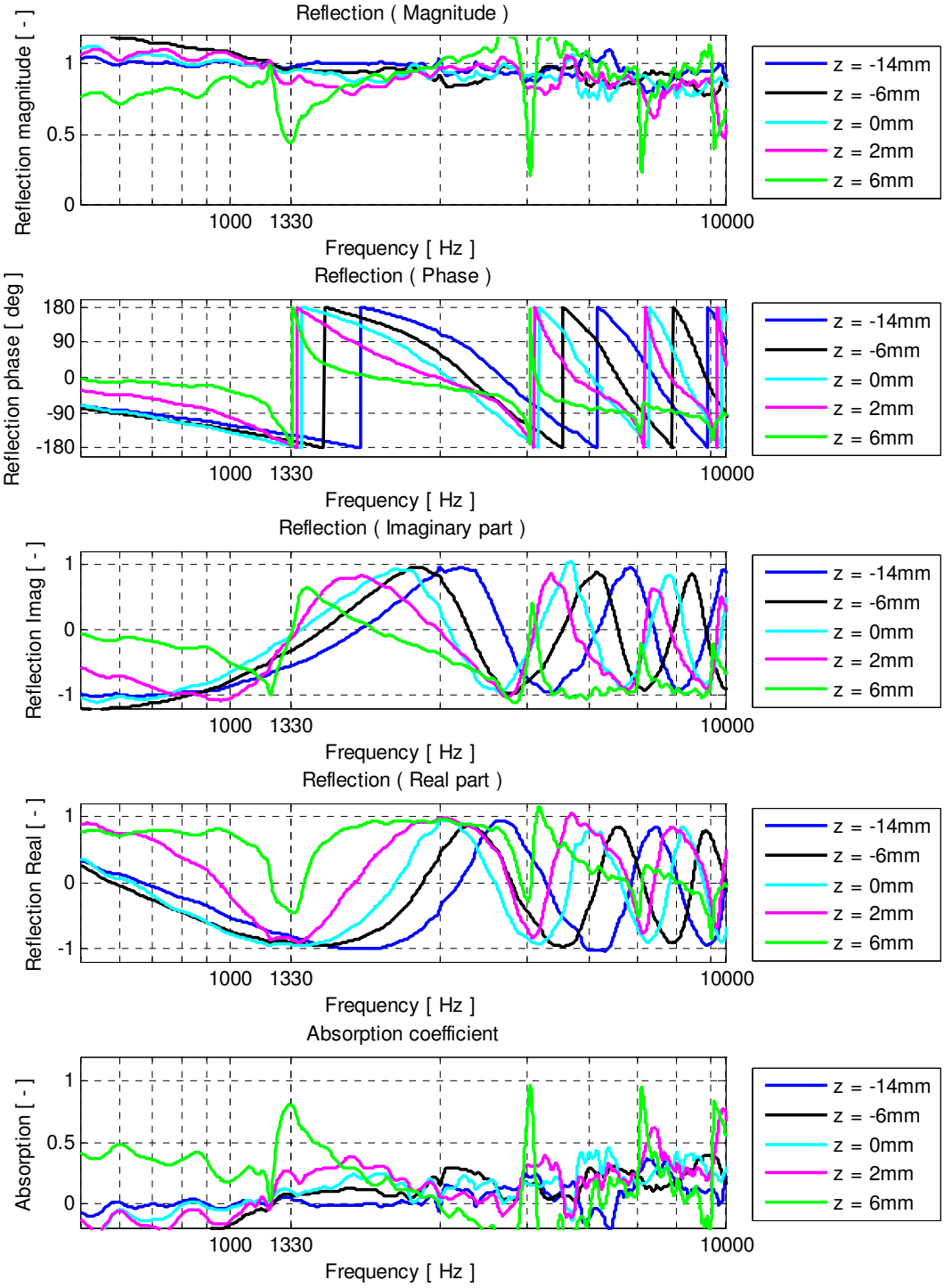

Fig. 6.56: Reflection and absorption along the z-axis (in and out the tube).

The pressure doesn't change much outside the tube, while there is a large pressure variation inside the tube. This might explain why it is difficult to estimate impedance outside a tube based on pressure measurements alone (e.g. Tamura method). And with enough dynamic range inside a tube it is possible (Kundt's tube method).

Kundt's tube reference

As a reference the same sample is also measured with the PU probe Kundt's tube method [1], [4], [5], see Fig. 6.57. The Kundt's tube has a 46 x 46 mm square profile and sound waves will travel only in one dimension below the cut-off frequency of 3500Hz. The plate with resonator can directly be mounted at the end of the Kundt's tube so there is no risk of re-positioning the sample and to change its acoustical properties.

The absorbing properties of a wall resonator is dependent of the ratio between the tube diameter and the distance between the tubes [8]. The measurement shows that one tube in a relatively large plate absorbs nearly all sound at one single frequency (1320 Hz). Nearly the same frequency as measured close to the tube with the local free field measurements (1330 Hz).

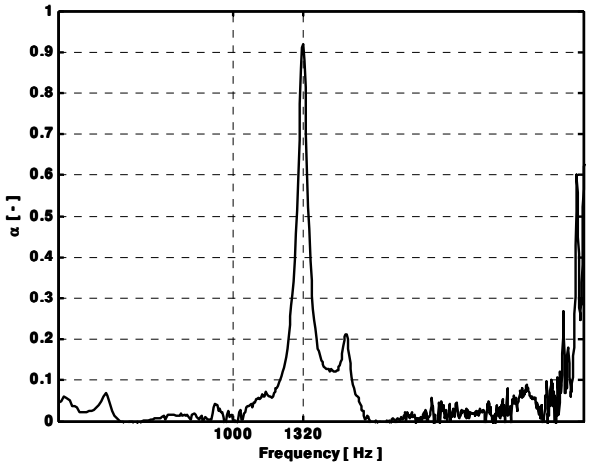

Fig. 6.57: Kundt's tube absorption of one quarter lambda resonator.

Three quarter lambda samples

The entire surface of the same sample, but now with three quarter lambda tubes is measured 3mm from the surface with a 5x5mm grid (81 measurements), see Fig. 6.58. Each tube will cause the sample to absorb at its particular resonant frequency.

Because each segment of the sample is observed, the combination of these measurements should represent the behavior of the total sample. The result can than be compared with the Kundt's tube.

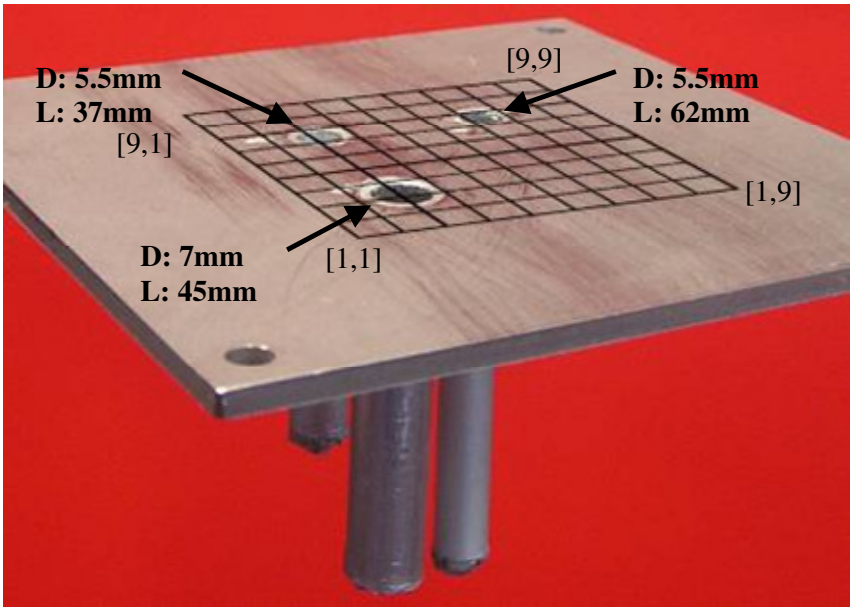

Fig. 6.58: Measurement grid of a sample with three quarter lambda resonators.

In the figures below the results are plotted at the 1st resonant frequency of each tube at respectively 1330, 1841 and 2218 Hz. Here it is shown that the real part of reflection goes to -1 above the corresponding tube. At that position the absolute reflection and absorption are zero.

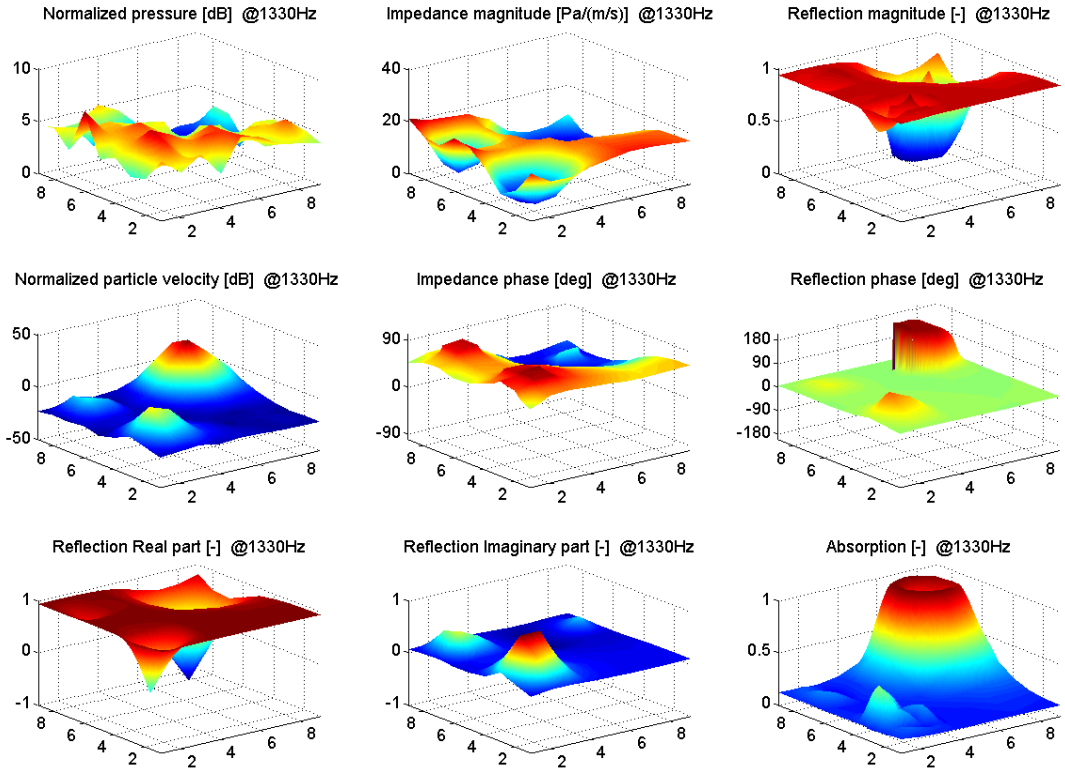

Fig. 6.59: Three tubes at 1330 Hz. The upper tube is most dominant (l = 62 mm), position [7,7]

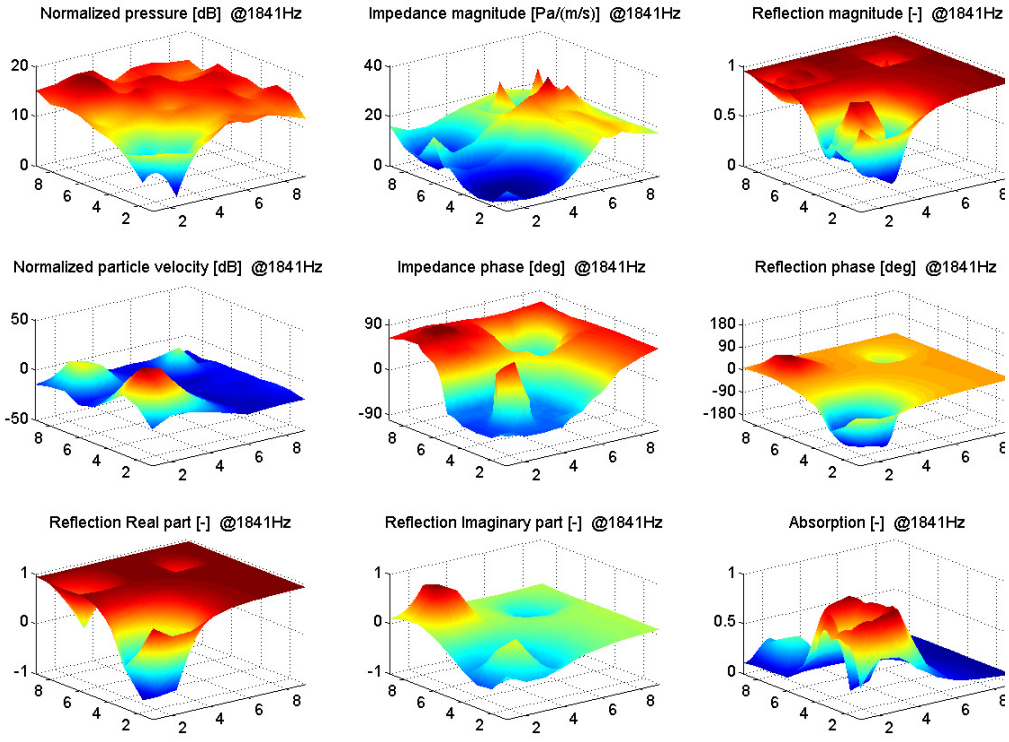

Fig. 6.60: Three tubes at 1841Hz. The lower tube is most dominant (l=45mm), position [3,3].

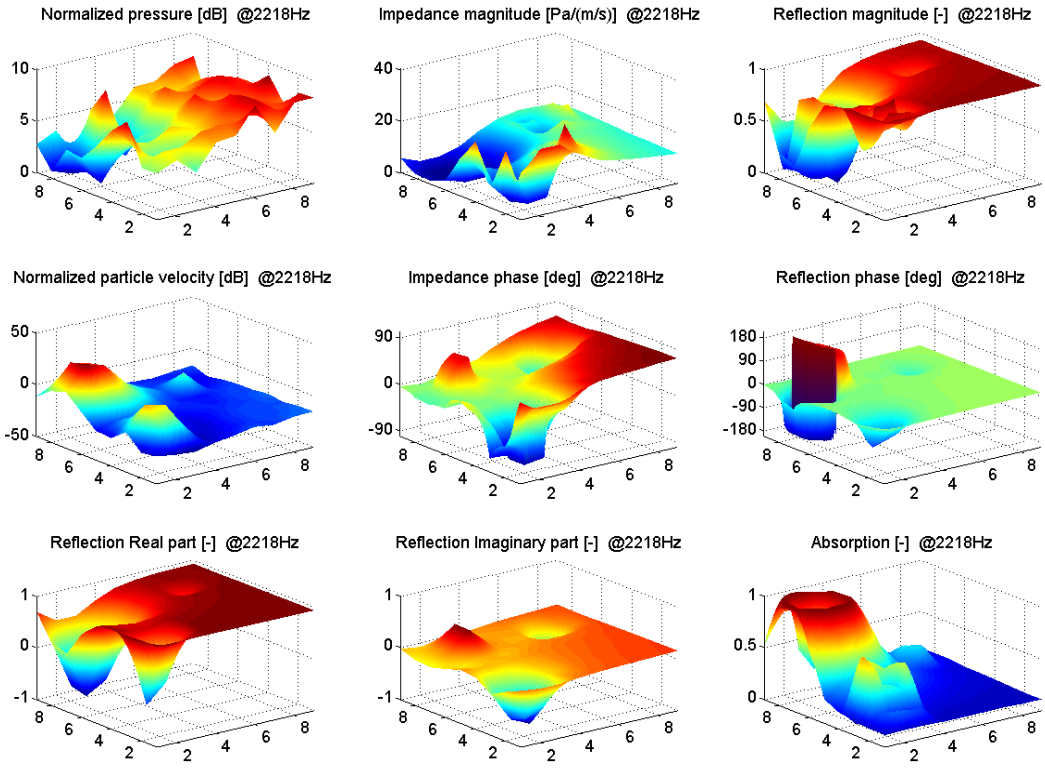

Fig. 6.61: Three tubes at 2218Hz. The lower tube is most dominant (l=37mm), position [7,3].

Kundt's tube comparison

With the averaged sound pressure and particle velocity value close to the plate the effective impedance of the covered surface can be calculated:

$$Z = \frac{\sum |p| e^{i\varphi_p}}{\sum |u| e^{i\varphi_u}} \tag{6.43}$$

With the effective impedance the reflection and absorption of the entire sample can be obtained. Fig. 6.62 shows the Kundt's tube and the effective impedance of the local measurements give a comparable result.

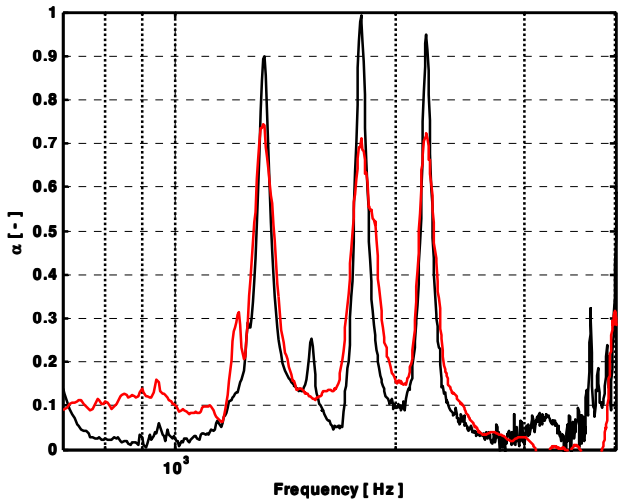

Fig. 6.62: Kundt's tube response of the 3 tubes sample (black line) and effective impedance of the local measurements (red line)

To avoid deviation due to sample positioning the plate is directly placed at the end of the Kundt's tube. Nevertheless the samples properties change because the sample area is affected in the Kundt's tube. The absorption value of a quarter lambda resonator in a wall is determined by the relation between tube diameter and the area around the tube. The unwanted modification of the sample area because of the Kundt's tube dimensions might explain the difference between the two methods at the peeks.

6.7. Measurements of a slotted panel absorber

A slotted and perforated panel absorber is the subject of investigation. This absorber is called "Topakustik-eco" and it is manufactured by the Fantoni Group in Italy. According to the manufacturer this absorber can be applied in walls and ceilings. The four commercial types of Topakustik-eco available are obtained by changing the size and spacing of the holes in the perforated panel.

The Topakustik-eco behaves like a perforated panel helmholtz absorber. In short, the perforated panel is an absorber consisted of a closed cavity, partially filled with porous material, which is closed on the top by a

perforated panel. The air in the holes takes the role of a mass vibrating over a spring, which is represented by the volume of air enclosed in the cavity. A mixture of acoustical losses, provided by the porous material, and phase changes, in the reflected pressure, are the causes of acoustical absorption.

The Topakustik-eco has a more complex behavior due to its construction. This complexity creates more resonances (peaks) in the absorption coefficient curve. According to the manufacturer the absorption characteristics of the Topakustik-eco can be changed depending on the mountings used. The configuration of the absorber, used in this paper, can be seen in Fig. 6.63. It is consisted of the Topakustik-eco sheet over a layer of porous material. This whole structure was applied over a hard surface. Measurements took place very close to the surface of the absorber. Many points were measured along an area of the absorber. Therefore, one can investigate how the absorption of the panel varies in space, and also calculate a spatial average of the acoustical surface impedance, reflection and absorption coefficients.

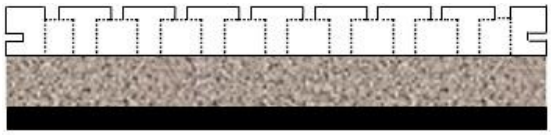

Fig. 6.63: Schematic drawing of the absorber.

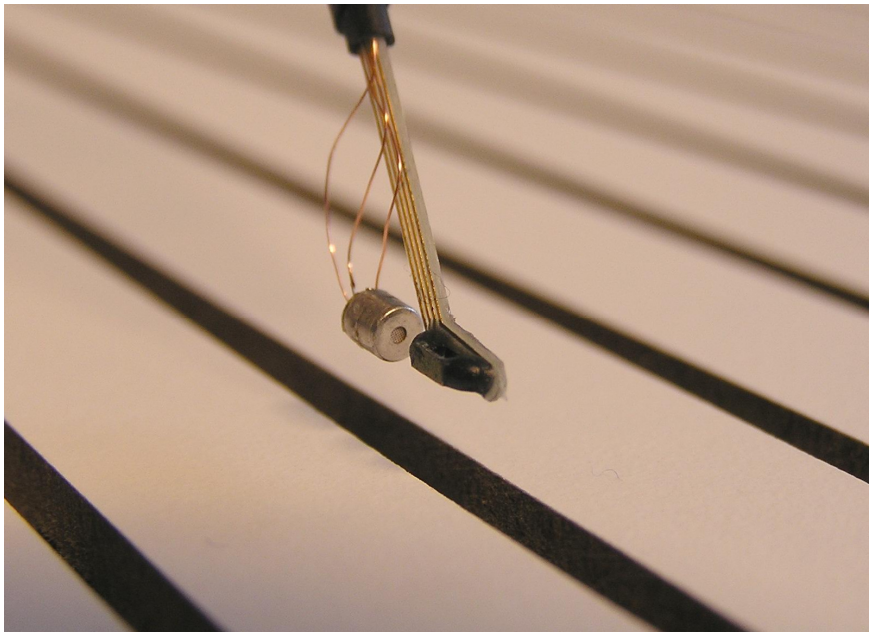

Fig. 6.64: Dedicated PU match probe close to the surface of the absorber.

Fig. 6.65 shows the typical behavior of a perforated panel absorber. It's possible to see a high absorption coefficient value around a resonant frequency (main peak - 1400Hz), and other resonances (peaks) and anti-resonances (valleys). Figure 6 shows that the absorption characteristics are caused by attenuation and phase changes in the reflected pressure field.

Near the main resonance (1400Hz) there is mainly attenuation in the reflected pressure field, as the phase of the reflection coefficient is close to zero degrees.

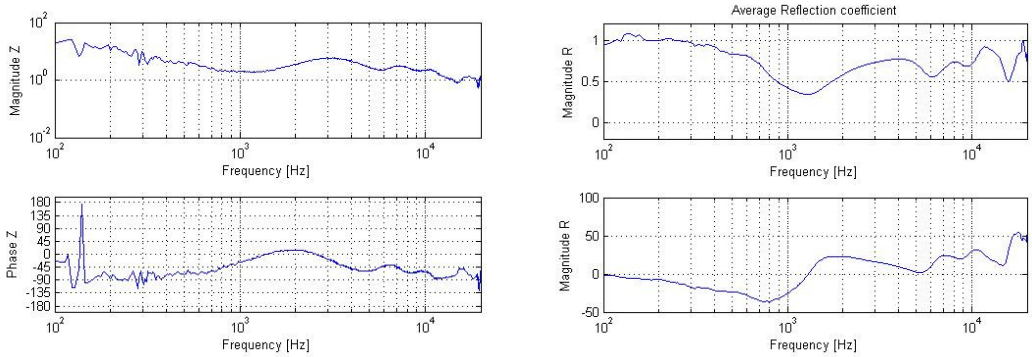

Fig. 6.65: dedicated PU match probe close to the surface of the absorber.

Another interesting result is how the absorption coefficient varies in space. One can see the absorption coefficient of 10 points along the scanned area of the absorber. It's easy to note that the contour of the absorption coefficient is similar for all the points showed (It was also noted for all the other points measured, but not all results are shown here). On the other hand, the value of the absorption increases or decreases depending on the measured point of the grid.

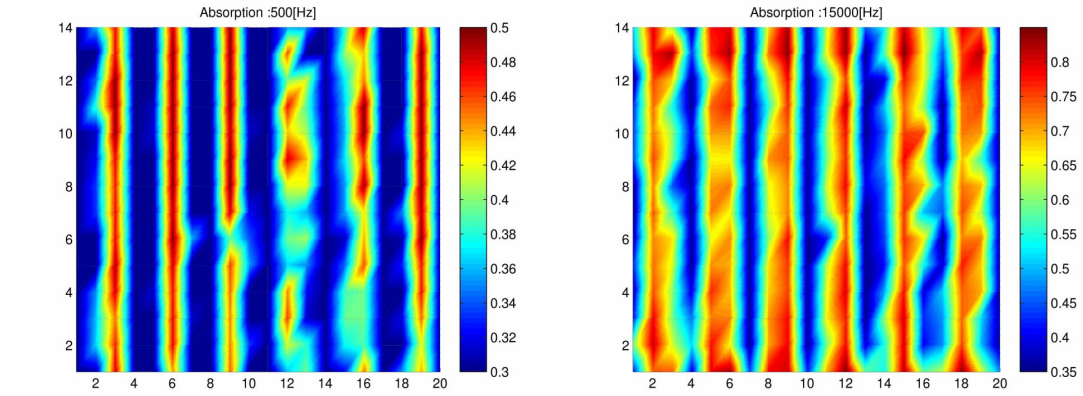

Fig. 6.66: Variation of the absorption coefficient in space (left: 500Hz, right: 1500Hz)).

It is suspected that measurements taken above the slots would lead to a higher absorption coefficient, while measurements taken above the hard reflecting part of the perforated panel would lead to a smaller absorption values. In order to investigate this, color maps of the absorption coefficient were plotted (one for each frequency). This way, it's possible to see how the absorption, in a certain frequency, changes across the area of the absorber. These color maps shows the local absorption coefficient, but do not describe the absorption of the sample as a whole.

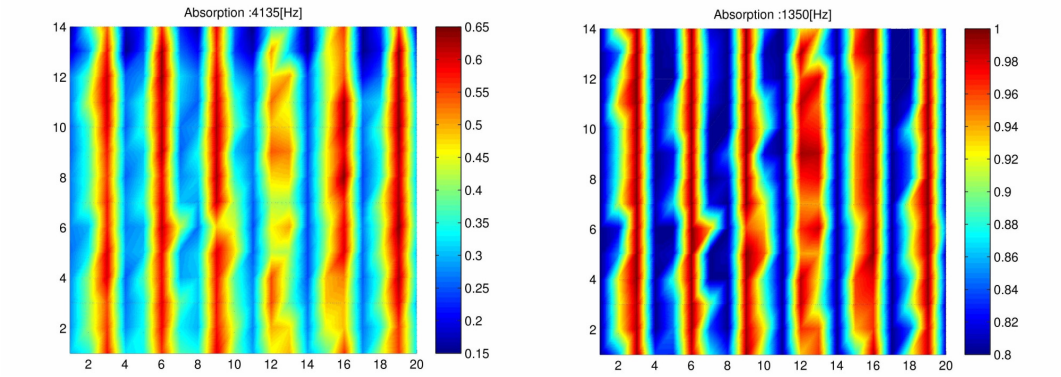

Fig. 6.67: Variation of the absorption coefficient in space (left: 4135Ha, right: 1550Hz)).

Impedance in the slot

The surface impedance is also investigate in the slots, see Fig. 6.68.

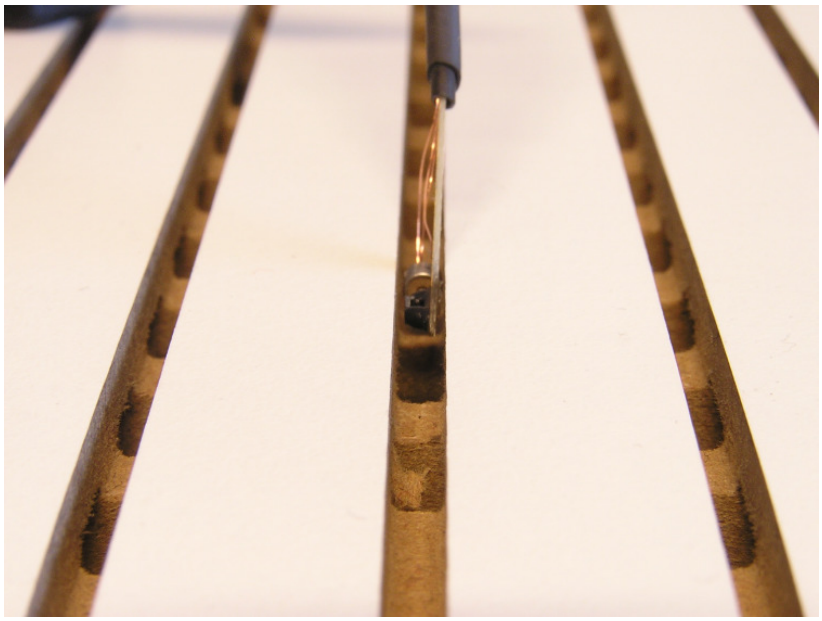

Fig. 6.68: Measurement in the slot.

Three different distances (from the perforations to the probe) were used. First it was measured very close to the holes (h=1mm). After that, measurements took place near the entrance of the slot. For last, measurements were taken at the same distance of the previous measurements. This last one was used only for comparison with the former measurements, in order to check the accuracy. This last result is not shown but was in agreement.

Ten points were measured for each one of these three distances. Five of this points above holes, and five above the reflecting surface in the slot (called here "non hole"). This way one can see if the magnitude of the impedance changes above the holes.

Fig. 6.69 shows these results for four points. One can see that there are no significant differences in the impedance measured above the hole and

reflecting surface. This is due to the fact that the distance from the pu probe to the perforations are relatively big, as these measurements were taken at the slot entrance. It shows that the magnitude of the impedance is smaller just above the holes (blue and red lines). This is due to the higher particle velocity values observed near the holes, which was expected due to the physical behavior of the perforated panel.

It's not possible although, to draw conclusions about the absorption characteristics of the whole panel with measurements taken in the slot. The absorption of the panel is caused by the interactions of the holes, slots and reflecting surfaces of the panel. So, measuring in the slot just points to variations of the particle velocity near the holes and not to the overall absorption characteristics of the panel. These measurements can give valuable insight about the impedance of the hole itself.

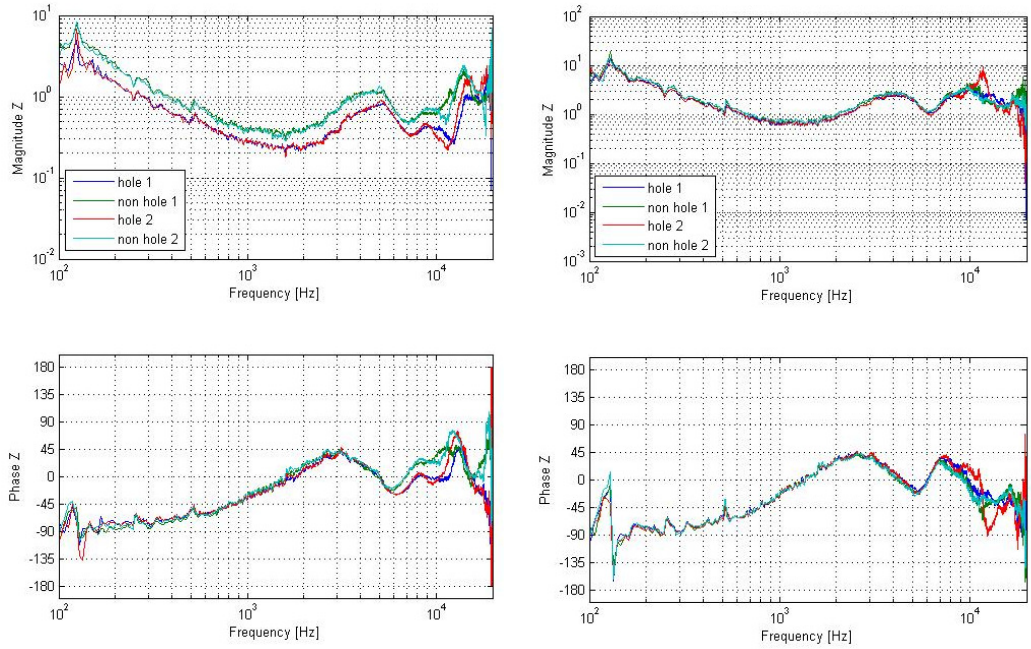

Fig. 6.69: Left: acoustic impedance in the slot, right: acoustic impedance in the slot entrance.

6.8. Measurement of the vocal tract impedance

A nice application of impedance measurements is the determination of vocal tract resonances. The technique uses a non-invasive acoustic excitation of the vocal tract and a fast and robust detection. The method can be used for patients with voice and speech disorders. Sweep signals (or white noise) are emitted and recorded simultaneously from the small end of a tube placed in front of the mouth opening. The use of a pressure sensor and a velocity sensor provides a direct measurement of the vocal tract impedance at the mouth [25]. It is also possible to determine the impedance of the mouth with a special acoustic source that produces a known particle velocity [24].

Key of the measurement is the measurement of the acoustic impedance of the vocal tract (mouth, throat etc.). For this an external noise source is needed because the glottis produces only sound with specific frequency components. If that noise is used, the impedance of the focal tract can only be determined partially. A white noise source is used to be able to determine a broad banded impedance result.

Once the impedance as function of the frequency is known, the first two resonances give an insight what vowel is pronounced, see Fig. 6.70 (right).

With this method it is possible to train people with hearing problems who lack the biofeedback that is needed to learn to pronounce vowels properly.

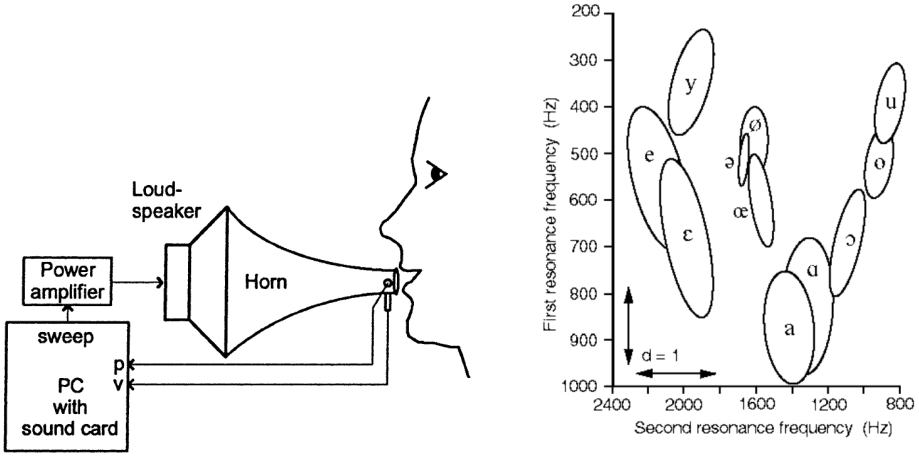

Fig. 6.70: Left: impedance measurement set up (from [25]). Right: the vocal tract resonances for seven adult female native speakers of French (from [24]).

6.9. The mirror source method

Measurements in a confined space are difficult with the surface impedance method. One of the difficulties is also that when the reflection coefficient equals unity, the particle velocity at the surface is zero. Apart from that, at highly reflecting surfaces, the method is sensitive for phase errors [23]. For highly reflective surfaces and measurements in confined spaced another method is developed.

The method is still in the R&D phase; it is not fully understood yet.

A monopole sound source *Q* is put close to an acoustic reflecting surface and the sound field can be modelled by the use of a mirror source *Q'*. A Microflown is placed close to the point source in such way that its sensitive direction is aiming at the mirror source and its non-sensitive direction is pointing towards the monopole sound source. It will therefore only 'see' the mirror source.

The sound field that the mirror source produces equals the sound field of that the monopole sound source times the reflection coefficient.

Because the particle velocity of only the mirror source is measured, the method works best for highly reflective materials. If the surface is highly absorbent, the particle velocity microphone is not measuring anything. In that sense it is a complementary method to the surface impedance method.

The particle velocity field of a monopole is given by (see also chapter 2 and chapter 9):

$$u(r,t) = \frac{Q'}{4\pi}\frac{ikr+1}{r^2}e^{i(\omega t-kr)} = R_s\frac{Q}{4\pi}\frac{ikr+1}{r^2}e^{i(\omega t-kr)} \tag{6.44}$$

The measured particle velocity is depending on the spherical reflection coefficient R_s, the distance r and the source strength.

As a reference measurement the particle velocity is measured at a certain distance r_1 from a fully reflecting surface.

The ratio given by the measurement done in the close proximity (r_2) of the acoustic sample and the reference measurement is given by:

$$\frac{u(r_2)}{u(r_1)\big|_{R=1}} = \frac{R_s\frac{Q}{4\pi}\frac{ikr_2+1}{r_2^2}e^{ikr_2}}{\frac{Q}{4\pi}\frac{ikr_1+1}{r_1^2}e^{ikr_1}} = R_s\frac{r_1^2}{r_2^2}\frac{ikr_2+1}{ikr_1+1}e^{ik(r_2-r_1)} \tag{6.45}$$

The only unknown is the measurement distance r_1 and r_2. As can be seen, if the measurement distance is kept constant (r_1=r_2), the ratio of the two velocity measurements is a direct measure for the reflection coefficient.

The measurement distance is clearly defined when measuring close to a rigid surface. The measurement distance may be difficult to obtain when measuring soft damping materials.

The measurement procedure consists of three steps:

Step 1: anechoic reference measurement

The setup is placed in an anechoic room and adjusted so that the particle velocity becomes minimal. Now the Microflown can almost not measure the loudspeaker output. Of course there is always some scattering or mechanical crosstalk so the Microflown output will not reach zero.

Step 2: calibration measurement

If the setup is placed close to a fully reflecting plate, the particle velocity that is measured equals:

$$u_{R=1} = \frac{Q}{4\pi}\frac{ikr_1+1}{r_1^2}e^{ikr_1} \tag{6.46}$$

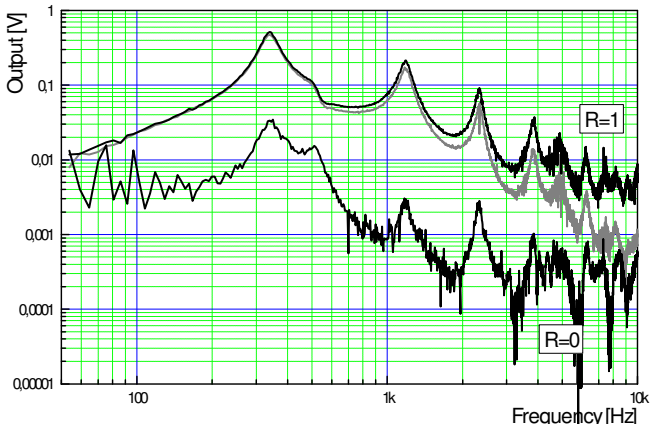

Fig. 6.71: Velocity output of the three steps. Upper (Black R=1) line: output close to a fully reflecting plate, middle (grey) line: output close to the acoustic material, lower (black R=0) line: anechoic output.

Step 3: measurement of acoustic sample

If the setup is placed close (and $r_1=r_2$) to a sound absorbing plate the particle velocity that is measured equals:

$$u_R = R\frac{Q}{4\pi}\frac{ikr_2+1}{r_2^2}e^{ikr_2} \tag{6.47}$$

The results of the three measurements are shown in Fig. 6.71.

The ratio between the anechoic reference response (step 1) and the response on fully reflecting plate (calibration measurement) is called the quality. This ratio gives the maximal dynamic measurement range of the method. A high ratio means that the zero adjustment of the particle velocity sensor versus point source is done well. The quality is shown in Fig. 6.72.

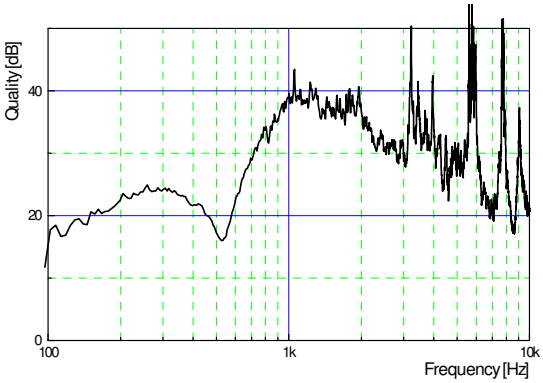

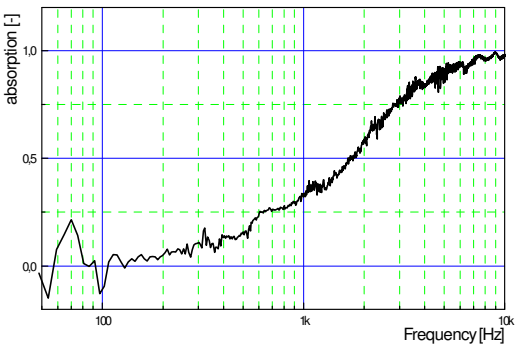

Fig. 6.72: Quality of the zero adjustment in the mirror source technique. Fig. 6.73: Absorption coefficient of a sample obtained with the mirror source technique.

The reflection coefficient of the measurement method is derived from the ratio of the measurement on the acoustic material and the calibration measurement (the measurement on the fully reflecting plate). Note that the

representation of this ratio in Fig. 6.71 is in dB. The resulting absorption curve is shown in Fig. 6.73.

In the preliminary R&D it showed that the first two samples (a damping material that is used in cars and melamine foam) had a perfect match with standing wave tube results. A lot of other materials did not match. The reason why is still under investigation.

The mirror source method, influence of sample size

To get an understanding of the required measurement areas a sample of 4cm Flamex (an open cell melamine foam) was measured, reduced in size and measured again. The procedure is repeated until the sample size was too small to be practical (the sample size is smaller than the thickness of the material).

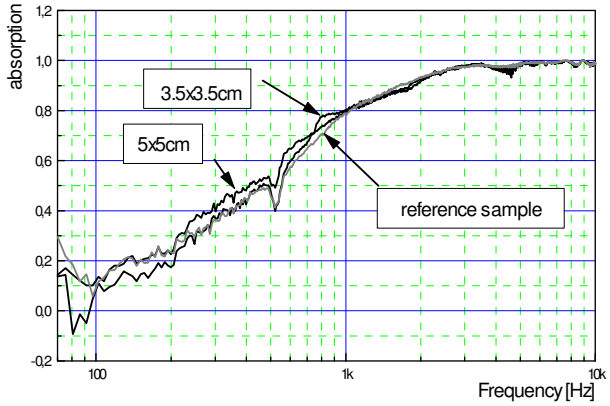

Fig. 6.74: The effect of sample size: an extremely small sample size is required for the mirror source technique.

The mirror source technique requires an extremely small sample size as can be seen in Fig. 6.74. A picture of the measurement of the 3.5x3.5cm sample is shown below (Fig. 6.75).

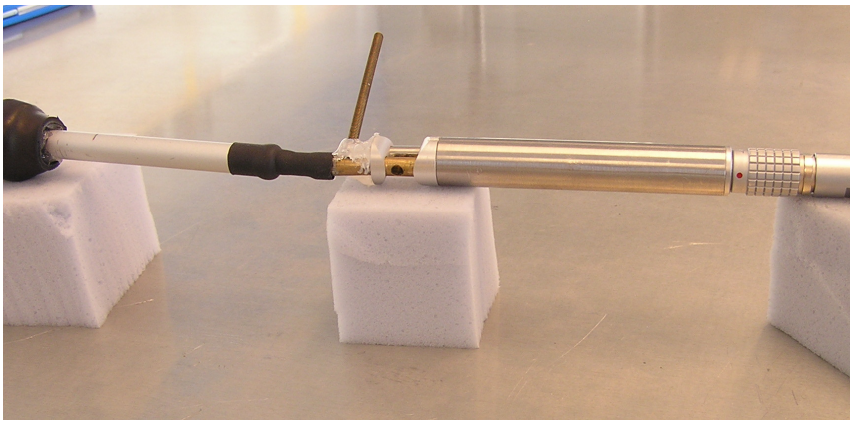

Fig. 6.75: An extremely small sample is measured with the mirror source technique. Left the driver for the point source is seen. The source is the little hole seen in the head of the pu probe.

The mirror source method, influence of environment

The acoustic properties of damping materials are traditionally measured in a laboratory. To test the methods how they hold up in real live situations a large (50x50cm) reflecting plate is put close to the set up. The results are discussed in this paragraph.

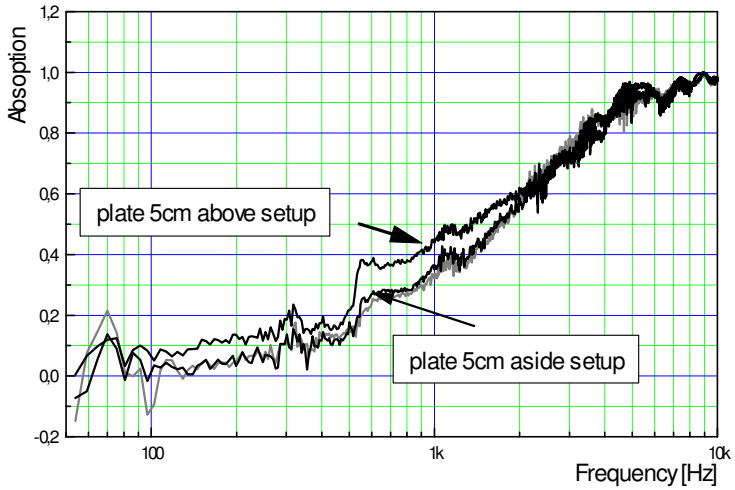

Fig. 6.76: Effect of an acoustic disturbing plate close to the mirror source technique.

To study the influence of the environment a highly reflecting plate was put 5cm horizontally above and 5cm vertically aside the setup to determine the environmental sensitivity. The effect of the plate is shown in Fig. 6.76.

As can be seen, a highly reflective plate placed 5cm vertically aside the set up does not the influence the measurement. A highly reflective plate placed 5cm above the set up does influence the measurement a bit.

6.10. References

[1] Thesis Frits van der Eerden, PhD thesis, University of Twente, Enschede, The Netherlands, November 2000, ISBN: 90-36515211.

[2] Schurer H., Annema P., de Bree H-E., Slump C.H., Herman O., Comparison of two methods for measurements of horn input impedance, J. Audio Eng. Society, 44, 649 (1996).

[3] Eerden, F.J.M., de Bree, H-E., Tijdeman, H. Experiments with a new acoustic particle velocity sensor in an impedance tube, Sensors and Actuators A, 69, 126-133 (1998).

[4] H-E. de Bree, F.J.M. van der Eerden, J.W. van Honschoten, A novel technique for measuring the reflection coefficient of sound absorbing materials, ISMA25, International Conference on Noise and Vibration, September 13-15, 2000 - Leuven, Belgium.

[5] R. Lanoye et al, Experience with different free field techniques to evaluate the surface impedance, ICA 2004.

[6] R. Lanoye et al, a practical device to determine the reflection coefficient of acoustic materials in-situ based on a Microflown and microphone sensor, ISMA, 2004.

[7] R. Lanoye et al, Measuring the free field acoustic impedance and absorption coefficient of sound absorbing materials with a combined particle velocity-pressure sensor, JASA 2006.

[8] M. A. Nobile and S. I. Hayek, Acoustic propagation over an impedance plane, JASA 78, 1325–1336, 1985.

[9] www.rieter.com (ALPHA_CAB[1].pdf)

[10] Rudnick, I., The propagation of an acoustic wave along a boundary, Journal of the Acoustical Society of America, 19, (1947), pp.348-356.

[11] F.J. Fahy, *"A simple method for measuring loudspeaker cabinet impedance,"* J. Audio Eng. Soc., Vol. 41, No. 3, pp. 154–156, (1993 March).

[12] Bree, H-E. de, Leussink, P.J., Korthorst, M.T., Jansen, H.V., Lammerink, T., Elwenspoek, M. The Microflown: a novel device measuring acoustical flows, Sensors and Actuators A, 54, 552-557 (1996).

[13] Tijdeman, H. On the propagation of sound waves in cylindrical tubes, J. of Sound and Vibration, 39(1), 1-33 (1975).

[14] Beltman, W.M. Viscothermal wave propagation including acousto-elastic interaction, part I: theory, J. of Sound and Vibration 227(3), 555-586 (1999).

[15] Bies, D.A., Hansen, C.H. Engineering Noise Control, theory and practice, E&FN SPON, London (1996).

[16] Fahy, F.J. Sound intensity, E&FN SPON, London (1995)

[17] Chung, J.Y., Blaser, D.A. (1980a). Transfer function method of measuring in-duct acoustic properties. I. Theory, Journal of the Acoustical Society of America, 68(3), 907-913.

[18] Chung, J.Y., Blaser, D.A. (1980b). Transfer function method of measuring in-duct acoustic properties. II. Experiment, Journal of the Acoustical Society of America, 68(3), 914-921.

[19] Chung, J.Y., Blaser, D.A. Transfer function method of measuring in-duct acoustic properties. I. Theory, J. of the Acoust. Society of America, 68(3), 907-913 (1980).

[20] Hans-Elias de Bree, Reinhilde Lanoye, Simon de Cock, Jos van Heck, Broad band method to determine the normal and oblique reflection coefficient of acoustic materials, SAE 2005

[21] De Bree, HE et al, An ultra miniature measurement tool to measure the reflection coefficient of acoustic damping materials in situ, SAE 2007.

[22] Stefan Weyna, the shapes of sound, acoustic wave flow visualisations in a real medium, 2006, ISBN 83-60140-58-8.

[23] Yang Liu and Finn Jacobsen, Measurement of absorption with a p-u sound intensity probe in an impedance tube, ASA, 2005

[24] A. Dowd, J. Smith and J. Wolfe, Learning to pronounce vowel sounds in a foreign language using acoustic measurements of the vocal tract as feedback in real time, Language and Speech, 41, 1-20 (1998).

[25] M. Kob, C. Neuschaefer-Rube, method for measurement of the vocal tract impedance at the mouth, Medical Engineering & Physics 24 (2002) 467–471

[26] M. Tamura, "Spatial Fourier-transform method for measuring reflection coefficients at oblique incidence. I. Theory and numerical examples," J. Acoust. Soc. Am. 88, 2259–2264 1990.

[27] M. Tamura, "Spatial Fourier-transform method for measuring reflection coefficients at oblique incidence. II. Experimental results," J. Acoust. Soc. Am. 97, 2255–2262 1995.

[28] E.H.G. Tijs et al, Non destructive and in situ acoustic testing of inhomogeneous materials, ERF33, Kazan, Russia, 2007.

[29] J.D. Alvarez, F. Jacobsen, In-situ measurements of the complex acoustic impedance of porous materials, INTER-NOISE 2007

[30] T.E. Vigran et al., Prediction and measurements of the influence of boundary conditions in a standing wave tube, Acta Acustica, 83, 419-423 (1997).

[31] HE de Bree, M. Nosko, E. Tijs, A handheld device to measure the acoustic absorption in situ, NVH GRAZ, 2008.

[32] M. Nosko, E. Tijs, HE de Bree, On the robustness of the PU surface impedance measurement technique, DAGA 2008.

[33] David B. Nutter et al., Measurement of sound power and absorption in reverberation chambers using energy density, JASA 2007

[34] Emiel Tijs, Hans-Elias de Bree, Piergiorgio Ferrante, Antonio Scofano, PU surface impedance measurements on curved liner materials in the presence of a grazing flow, CEAS, Bilbao, 2008

[35] Acoustic absorption measurements of moving structures and under influence of flow, Emiel Tijs and Hans-Elias de Bree, ISMA, 2008